Characterisation of organoclays and adsorption of p-nitrophenol: Environmental application

Yuri Park, Godwin A. Ayoko, and Ray L. Frost *

Chemistry Discipline, Faculty of Science and Technology, Queensland University of Technology, GPO 2434, Brisbane Queensland 4001, Australia

---

Abstract

Organoclays were synthesised through ion exchange of a single surfactant for sodium ions, and characterised by a range of method including X-ray diffraction (XRD), BET, X-ray photoelectron spectroscopy (XPS), thermogravimetric analysis (TGA), Fourier transform infrared spectroscopy (FT-IR), and transmission electron microscopy (TEM). The change in surface properties of montmorillonite and organoclays intercalated with the surfactant, tetradecyltrimethylammonium bromide (TDTMA) were determined using XRD through the change in basal spacing and the expansion occurred by the adsorbed p-nitrophenol. The changes of interlayer spacing were observed in TEM. In addition, the surface measurement such as specific surface area and pore volume was measured and calculated using BET method, this suggested the loaded surfactant is highly important to determine the sorption mechanism onto organoclays. The collected results of XPS provided the chemical composition of montmorillonite and organoclays, and the high-resolution XPS spectra offered the chemical states of prepared organoclays with binding energy. Using TGA and FT-IR, the confirmation of intercalated surfactant was investigated. The collected data from various techniques enable an understanding of the changes in structure and surface properties. This study is of importance to provide mechanisms for the adsorption of organic molecules, especially in contaminated environmental sites and polluted waters.

Keywords – Organoclay, X-ray photoelectron spectroscopy, montmorillonite, surfactant, BET

* Corresponding author: Ray L. Frost
Email address: g. r.frost@qut.edu.au
Address: 2 George Street, Brisbane Q 4001, Australia

Introduction

Clay minerals such as montmorillonite and smectite are abundant in nature. Clay minerals are known as the swelling clays due to their tendency to swell and hydrate upon exposure to water [1]. They are widely used in a variety of industries such as nano composites, catalysts, photochemical reaction reagents, and adsorbents [2]. Among other applications, clays have extensively been used as adsorbents in environmental systems, and the most commonly used clay is montmorillonite because of its high cation exchange (CEC), swelling properties, high surface areas, and consequential strong adsorption/absorption [3, 4]. Montmorillonite is a typical 2:1 layered clay mineral that consists of two inward pointing tetrahedral sheets with a central alumina octahedral sheet. The negatively charged clay layer surface is counterbalanced by exchangeable cations such as Na^{+} or Ca^{2+} in the interlayer space due to the isomorphous substitution within the layers (e.g. the replacement of Mg^{2+} or Zn^{2+} for Al^{3+} in the octahedral layer, and Al^{3+} for Si^{4+} in the tetrahedral sheets) [4, 5]. Because of the hydration of inorganic cations on the exchange sites, the clay mineral surface is hydrophilic in nature and this makes the natural clays ineffective sorbents for the removal of organic compounds. Such a difficulty has been overcome through ion exchange of inorganic cations with organic cations such as quaternary ammonium cations (QACs), represented as $[(CH_3)_3NR]^{+}$, or $[(CH_3)_2NR_2]^{+}$, where R is a relatively short hydrocarbon substitution group.

By introducing cationic surfactant molecules into the interlamellar space through ion exchange, the properties of clay minerals are changed from montmorillonite to organoclays. The intercalation of cationic surfactant between clay layers exchanges the surface properties from highly hydrophilic/lyophobic to increasingly hydrophobic/lipophilic [6]. As a result of the modification of the properties of the swelling clay, the basal spacing in the layer increases and new sorption sites of clays are exposed. Such changes in the properties of the surfactant are important for the application of organoclays, and their significance in hydrophobic organoclay is highlighted by their use for water purification. To date, the application of organoclays to remove various organic compounds has been reported, and relative to untreated clays, the adsorption capacity for the removal organic contaminants has been improved by using organoclays [7-9].

In this study, tetradecyltrimethylammonium bromide (TDTMA) surfactant is used as an example of a long alkyl cationic surfactant for the preparation of organoclays, since the effect of the long alkyl surfactant with different loadings may increase the utilisation utility of the

63 modified clays. The present work was undertaken to investigate the changes of structure and
64 physical properties in the modified clays, and the interlayer configuration of intercalated
65 surfactant in montmorillonite was elucidated by using X-ray diffraction (XRD), transmission
66 electron microscopy (TEM), Brunauer, Emmett, and Teller (BET), thermogravimetric
67 analysis (TGA) and Fourier transform infrared spectroscopy (FT-IR). In addition, using X-
68 ray photoelectron spectroscopy (XPS), the surface characteristics of montmorillonite and
69 organoclays were investigated. As many literature articles have reported the effectiveness of
70 organoclays as adsorbents, this study will further investigate any structural or physical
71 changes, or adsorption properties of the resultant organoclays when intercalated with organic
72 compounds. P-nitrophenol was chosen as a test molecule in this research. The obtained
73 results will offer new insights into the structure and adsorption properties of organoclays, and
74 will enhance the potential industrial applications of organoclays as a filter material in water
75 purification.

76

77 **Experimental Methods**

78 **Materials**

79 The pure montmorillonite (MMT) was purchased from Sigma-Aldrich, and was used
80 without further purification. The cation exchange capacity (CEC) of this pure
81 montmorillonite is 76.4 meq/100g (according to the specification of its producer). The
82 surfactant selected for the organoclay complexes in this study is
83 tetradecyltrimethylammonium bromide (denoted as TDTMA, $C_{17}H_{38}NBr$, FW: 336.41) from
84 Sigma-Aldrich, and used without any further purification.

85

86 **Synthesis of Organoclays**

87 The synthesis of organoclay complexes was undertaken by the following procedure: 4 g of
88 montmorillonite was initially dispersed in 400 mL of deionised water with a Heidolph
89 magnetic stirrer for about 30 minutes. A predissolved stoichiometric amount of surfactant,
90 which was dissolved in 100 mL of deionised water was stirred for a further 30 minutes. The
91 dissolved surfactant was slowly added to the clay suspension at room temperature (about 28 ~
92 30 °C). The CEC of the montmorillonite is 76.4 meq/100g, which represents a measure of the

loading of the clay with the cationic surfactant. For instance, 1.0 CEC is applied when 76.4 meq/100g is intercalated into the montmorillonite. During the synthesis, a range of surfactant concentration in terms of the CEC value from 0.25 CEC through 2.0 CEC was prepared and labelled as 0.25 CEC-TDTMA, 0.5 CEC-TDTMA, 1.0 CEC-TDTMA, 1.5 CEC-TDTMA, and 2.0 CEC-TDTMA. The mixtures were stirred for 3 hours at room temperature using a Branson Ultrasonic model 250 sonifier with an output of 40 mW. All organoclay products were washed free of bromide anions as determined by the use of the $AgNO_3$, dried at room temperature, and dried further in an oven (at 65 °C) for 12 hours. The dried organoclays were ground in an agate mortar, and stored in a vacuum desiccators for a week.

Adsorption of p-nitrophenol on the organoclays

0.2 g of the prepared organoclay products were combined with 30 mL of p-nitrophenol solution (4000 mg/L for the adsorption) in 50 mL centrifuged tube with plastic caps. The tubes were shaken for 6 hours at 190 rpm on a shaker at the room temperature. The initial pH of p-nitrophenol is 6.0. After shaking, the mixture was centrifuged at 3500 rpm for 20 minutes. After the centrifugation, the p-nitrophenol concentration in the aqueous phase was determined by a UV-Vis spectrophotometer at 317 nm with a detection limit of 0.05 mg/L.

The p-nitrophenol uptake on montmorillonite and/or organoclays was calculated by the following equation: $Q = (C_o - C_e) \cdot V / m$, Q is the uptake of p-nitrophenol, C_o is the initial concentration, C_e is the equilibrium concentration, V is the volume of p-nitrophenol solution and m is the mass of the adsorbent. The losses of the p-nitrophenol by both photochemical decomposition and volatilisation were found to be negligible during adsorption [9]. The obtained montmorillonite and organoclays adsorbed with p-nitorphenol were labelled as montmorillonite-4000, 0.25 CEC-4000. 0.5 CEC-4000, 1.0 CEC-4000, 1.5 CEC-4000 and 2.0 CEC-4000.

Characterisation methods

X-ray diffraction (XRD)

The pure montmorillonite and synthesised organoclays were pressed in stainless and samples holders. Powdered X-ray diffraction (XRD) patterns were recorded using CuKα

radiation (λ = 1.54Å) on a Philips PAN analytical X'pert PRO diffractometer operating at 40 kV and 40 mA with 0.25° divergence slit, 0.25° anti-scatter between 5 and 15° (2θ) at a step size of 0.0167°. For XRD at low angle section, it was between 1.5 and 8° (2θ) at a step size of 0.0167° with variable divergence slit and 0.125° anti-scatter. In addition, the organoclays adsorbed p-nitrophenol was applied as the same method prior to powder XRD analysis.

Transmission electron microscopy (TEM)

A JEOL 1010/2100 transmission electron microscopy was used to investigate microstructure of organoclays. All samples were ultrasonically dispersed in absolute ethanol solution and a small drops of suspension dissolved in ethanol solution was prepared on carbon-coated films and dried in an oven at 60 °C for 20 mins for TEM studies.

Brunauer, Emmett, and Teller (BET)

With a Micromeritics Tristar 3000 automated gas adsorption surface area analyses based upon N_2 adsorption/desorption were carried out. From the measurement, pore structure parameters were characterised at liquid nitrogen temperature. Before the measurement, the samples were pre-heated at 90 °C under the flow of N_2 on a Micrometrics Flowprep 060 degasser.

X-ray photoelectron spectroscopy (XPS)

The X-ray photoelectron spectroscopy (XPS) was applied using a Kratos AXIS Ultra with a monochromatic Al X-ray source at 225W. A small amount of each fine powdered sample was applied to the double sided adhesive tape on a standard Kratos Axis sample bar. This was attached to the sample rod of the Load Lock system for initial evacuation to 10^{-6} Torr. The sample bar was then transferred to the UHV sample analysis chamber (SAC) for collection of X-ray photoemission spectra. A survey scan was run for each analysis from 0 to 1200eV with a dwell time of 100 ms, pass energy of 160 eV at step of 1 eV with one sweep. In addition, a high resolution analysis was undertaken at 40 eV at steps of 50 meV. The obtained spectra

were analysed using Casa XPS version 2.3.14 software, which enabled the baseline (Shirley baseline applied) and various data handling procedures.

Thermogravimetric analysis (TGA)

Thermogravimetric analysis of the pure montmorillonite and synthesised organoclays were obtained by using TA instruments Inc. Q500 high-resolution TGA operating at ramp 5 °C/min with resolution 6.0 °C from room temperature to 1000 °C in a high purity flowing nitrogen atmosphere (40 cm^3/min). Approximately 40 ~ 60 mg of finely dried ground sample were heated in an open platinum crucible.

Fourier transform infrared spectroscopy (FT-IR)

Fourier transform infrared spectroscopy (FT-IR) was applied in this work, and the spectra were obtained using a Nicolet Nexus 870 FT-IR spectrometer with a smart endurance single bounce diamond ATR cell. Sixty four scans were collected for each measurement over the spectral range of 550 ~ 4000 cm^{-1}. Spectral manipulation such as baseline adjustment, smoothing, and normalisation were performed by using the GRAMS software package (Galactic Industries Corporation, Salem, NH, USA). Band component analysis was undertaken using the Jandel 'Peakfit" software package, which enables the type of fitting function to be selected and allows specific parameters to be fixed or varied accordingly. Band fitting was performed using a Lorentzian-Gaussian cross-product function with the minimum number of component bands used for the fitting process. The peak fitting was produced squared correlation (R^2) greater than 0.991.

Results and Discussion

X-ray diffraction (XRD)

X-ray diffraction (XRD) is one of the most useful techniques to probe the structural geometry and texture of organoclays. The basal spacing information of organoclays obtained from XRD provides the intercalation and molecular structure configuration of the organic surfactant into the clay layers. The XRD patterns of montmorillonite, and organoclays

prepared at different surfactant loadings with and without adsorbed p-nitrophenol are presented in Figures 1 and 2. The increasing basal spacing of untreated montmorillonite and organoclays is clearly seen Figures 3 and 4.

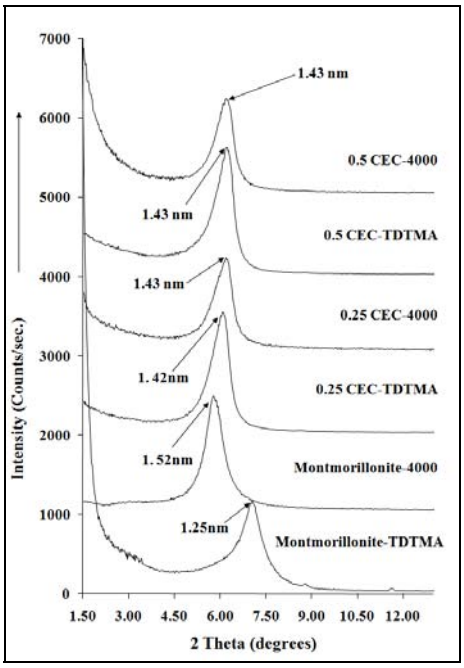

Figure 1. XRD patterns of montmorillonite, 0.25 CEC, and 0.5 CEC with and without adsorbed p-nitrophenol

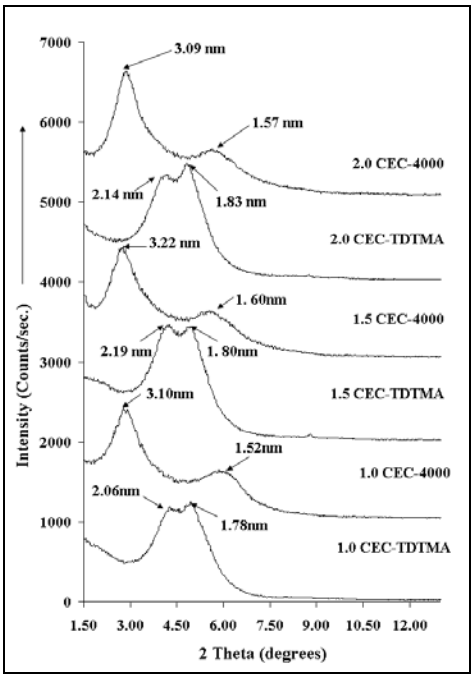

Figure 2. XRD patterns of 1.0 CEC, 1.5 CEC, and 2.0 CEC with and without adsorbed p-nitrophenol

189 The sodium exchanged montmorillonite has a d-spacing of 1.25 nm, which was expanded to
190 1.52 nm upon adsorption of p-nitrophenol. This expansion indicated that p-nitrophenol is
191 adsorbed between the clay layers. For an ion exchanged of 0.25 CEC surfactant concentration
192 level, a basal spacing of 1.42 nm is observed, and the value of 1.43 nm is observed upon the
193 adsorption of p-nitrophenol. The basal spacing of 1.43 nm is observed at the 0.5 CEC-
194 TDTMA and the expansion remains at 1.43 nm after adsorption of p-nitrophenol on the 0.5
195 CEC organoclay. Upon increasing the surfactant loading to 1.0 CEC surfactant concentration,
196 two d(001) spacings (1.78 nm and 2.06 nm) are observed, and there are two spacings at 1.52
197 and 3.10 nm observed upon adsorption of p-nitrophenol. At 1.5 CEC surfactant concentration
198 level, the organoclays also have the double overlapping expansion peaks at 1.80 and 2.19 nm,
199 which have a slightly more intense peak than that of organoclays at 1.0 CEC surfactant
200 concentration level. Upon adsorption of p-nitrophenol, the d spacing changed to 1.60 and
201 3.22 nm, respectively. The basal spacings at 2.0 CEC resulted in basal spacings of 1.83 and
202 2.14 nm. Where upon adsorption of p-nitrophenol, spacings of 1.57 and 3.09 nm are observed.
203 Depending on the concentration of surfactant (TDTMA), the expansion of the layers in each
204 step occurred. Based on the result, the configuration of the structure of the molecules between
205 clay unit layers is suggested.

206 In 0.25 CEC-TDTMA and 0.5 CEC-TDTMA, the d values are 1.42 and 1.43 nm,
207 respectively, and this implies monolayer arrangement in the interlayer space of
208 montmorillonite. From 1.0 CEC-TDTMA to 2.0 CEC-TDTMA, the two basal spacings at
209 1.78 nm (with a shoulder of 2.06 nm), 1.80 nm (with a shoulder of 2.19 nm) and 1.83 nm
210 (with a shoulder of 2.14 nm) indicate the two arrangement of the TDTMA surfactant
211 molecule within the clay mineral layers; the first basal spacing of 1.78 nm, 1.80 nm, and 1.83
212 nm is attributed to the arrangement of the surfactant molecule within the clay layers either
213 flat or perpendicular to the clay siloxane surface, while 2.06 nm, 2.19 nm, and 2.14 nm basal
214 spacings are ascribed to the surfactant molecules at right angles to the clay mineral surface.
215 Hence, at the higher CEC values from 1.0 to 2.0 CEC, both lateral bilayer and pseudo-
216 trimolecular layer structures of surfactant are observed. Upon adsorption of p-nitrophenol on
217 the organoclay the basal spacing for untreated montmorillonite was a slight expansion of the
218 clay layers from 1.25 nm to 1.52 nm, while 0.25 CEC-4000 and 0.5 CEC-4000 organoclays
219 both have spacing of 1.43 nm. This unchanged value may suggest that p-nitrophenol has
220 penetrated and bonded to the surfactant molecules in the clay layers. However, for the 1.0
221 CEC-4000 organoclays, there are two distinct basal spacings at 1.52 and 3.10 nm. The first

spacing of 1.52 nm is assigned to the organoclay with minimal p-nitrophenol adsorption, while the expansion of 3.10 nm is assigned to surfactant molecules with adsorbed p-nitrophenol between clay layers. Similar values of basal spacings are also observed upon reaching the 1.5 CEC-4000. By comparison with the previous studies by Xi et al.,[10] and Liu et al.,[11] similar configuration changes were obtained. As the surfactant concentration increased, the configuration structure changes from a lateral monolayer to lateral bilayer/pseudo-trimolecular layer structure were formed. However, the paraffin layer arrangement was not observed at the higher surfactant concentration in this study, and this may be due to the different molecular sizes of the surfactants. In addition, this result may be affected by the differences in the measurements and in the control humidity.

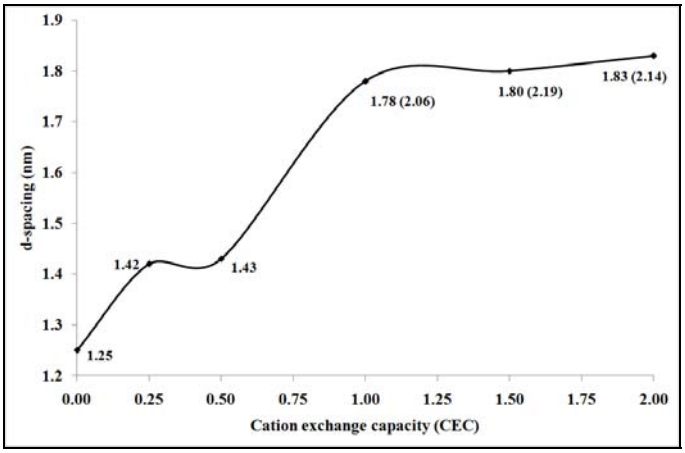

Figure 3. d(001) basal spacing of montmorillonite and organoclays

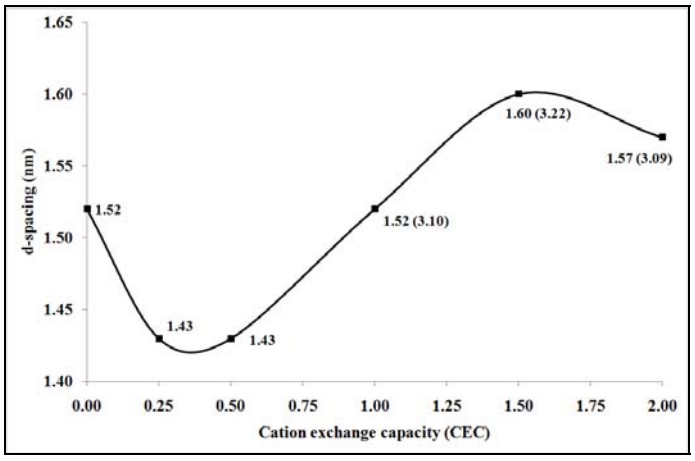

Figure 4. d(001) basal spacing of montmorillonite and organoclays with adsorbed p-nitrophenol

Transmission electron microscopy (TEM)

A selection of TEM images of 0.5 CEC-TDTMA, 2.0 CEC-TDTMA, 0.5 CEC-4000, and 2.0 CEC-4000 organoclays are present in Figure 5. The images of 0.5 CEC-TDTMA shows that the spacing of 1.44 nm, which is in good agreement with the value of 1.43 nm obtained from XPD data. The 0.5 CEC-4000 shows that the spacing of 1.48 nm, which is slightly bigger than the spacing of 1.44 nm measured by XRD. There are multiple interlayer spacings are found at 2.20, 2.15, 1.85, 1.80 nm for 2.0 CEC-TDTMA. In comparison with the value of 2.14 and 1.83nm obtained from XRD, there are similar spacings obtained. In addition, upon the adsorption of p-nitrophenol, 2.0 CEC-4000 has also several spacings at 1.32, 1.50, 1.52, 1.78, and 3.02 nm. The observed 3.02 and 1.52 nm are well matched with that of XRD values. Compared to TEM, where various basal spacings were observed, only average were shown by XRD. From the results of the TEM technique, it is proposed that layers are not only linear but also curved or bent. Due to the ununiformed structure, several different interlayer spacings within organoclays are observed.

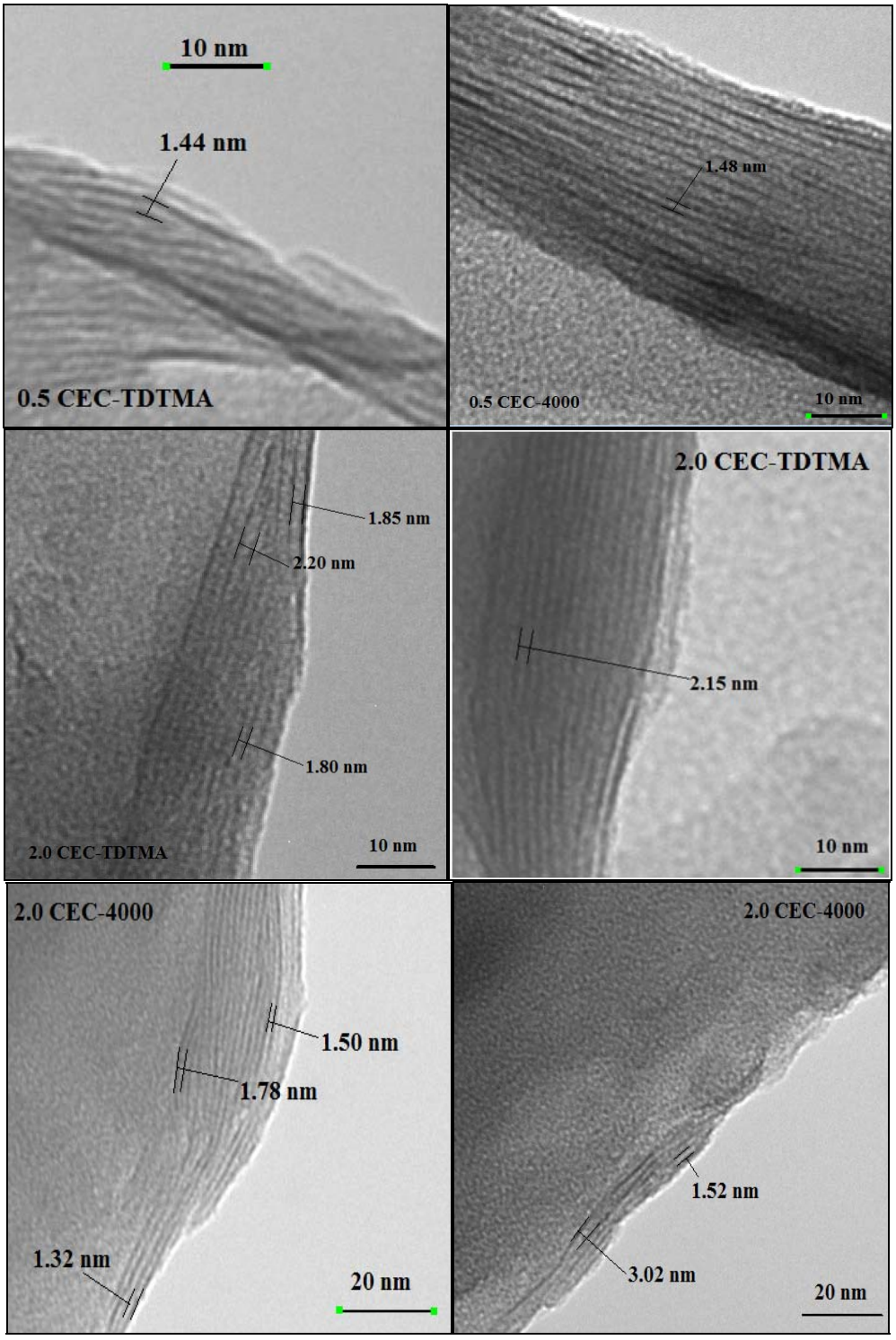

Figure 5. TEM images of 0.5 CEC-TDTMA, 2.0 CEC-TDTMA, 0.5 CEC-4000, and 2.0 CEC-4000

Surface area measurement

The BET method, the N_2 adsorption-desorption measurements of the clay and organoclays, was used to study the porosity and textual properties at liquid N_2 temperature. The results are shown in Figure 6. The Figure indicates that N_2 adsorption isotherms of clay and organoclays exhibit a Type II sorption behaviour in the classification of Brunauer, Deming, Deming and Teller (BDDT) [12]. It is clearly seen that the same form of isotherms and hysteresis loop are seen in both montmorillonite and organoclays. The large uptake of nitrogen is observed close to the saturation pressure, and this apparent step in adsorption branch with a sharp decline in the desorption branch implies the presence of mesoporosity [13-15]. This is in agreement with the pore diameter calculated from the Barrett-Joyner-Halenda (BJH) desorption isotherm as shown in Table 1. As shown in Figure 6, the adsorption of N_2 of montmorillonite is much higher than that of the other organoclays. This indicates that montmorillonite possesses a higher specific surface area. It is known that the specific surface area (S_{BET}), pore volume (V_p), and pore size distribution can be calculated and the calculated parameters are summarised in Table 1.

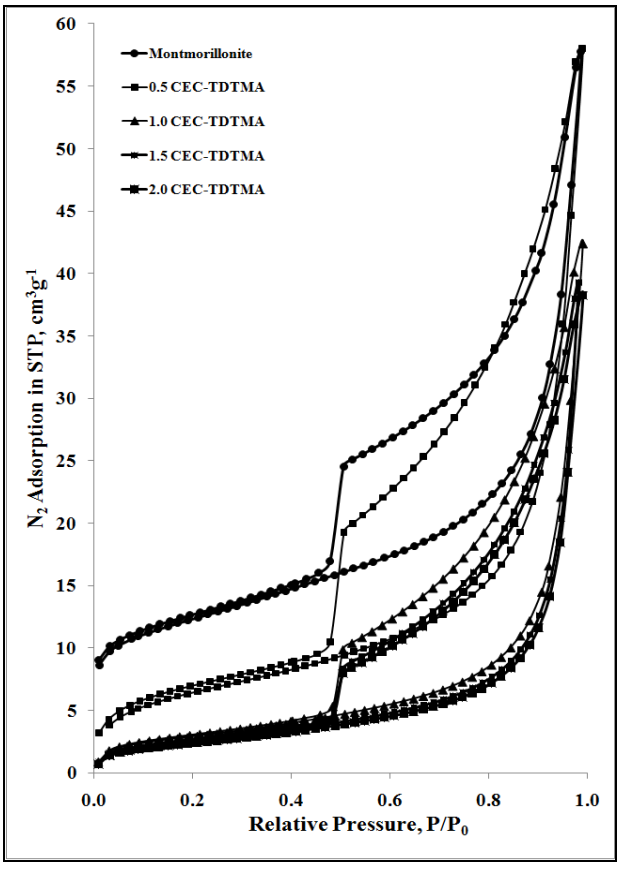

Figure 6. Nitrogen adsorption-desorption isotherms of montmorillonite and organoclays

278 **Table 1** BET specific surface area (S_{BET}), pore volume (V_p) and pore diameter for
279 montmorillonite and organoclays

Sample ID	S_{BET}, $m^2 \cdot g^{-1}$	V_P,[a] $cm^3 \cdot g^{-1}$	Mean D, nm	
			BET[b], nm	BJH[c], nm
Montmorillonite	42.7074	0.089560	8.3644	7.6372
0.5 CEC-TDTMA	23.7631	0.086054	14.5296	7.2432
1.0 CEC-TDTMA	10.8419	0.065352	24.2003	8.2589
1.5 CEC-TDTMA	9.4323	0.060594	25.7665	8.6636
2.0 CEC-TDTMA	8.8507	0.059009	26.7219	8.7463

280 [a] BJH desorption cumulative pore volume of pores between 1.7 and 300 nm in diameter.
281 [b] Adsorption average pore diameter (4*V*/*A* by BET).
282 [c] Barrett-Joyner-Halenda (BJH) desorption average pore diameter (4*V*/*A*).

283

284 As shown in Table 1, the BET surface area of montmorillonite and organoclays decreases
285 in order: Montmorillonite>> 0.5 CEC-TDTMA > 1.0 CEC-TDTMA > 1.5 CEC-TDTMA >
286 2.0 CEC-TDTMA. Especially, the surface area drops dramatically from montmorillonite to
287 0.5 CEC-TDTMA. It is also found that the pore volume for organoclays decreases with an
288 increase of loaded surfactants and this will be further discussed using TGA results. The pore
289 size is also related to the loading of surfactant, and organoclays with high surfactant loadings
290 have an enlarge pore size than that with low surfactant loadings. As shown in Table 1, using
291 specific surface area and pore volume, there are two different groups made. The surfactant
292 loading concentration up to 0.5 CEC-TDTMA with 23.7631 m^2/g and pore volume of
293 0.086054 cm^3/g. The other group includes 1.0 CEC-TDTMA to 2.0 CEC-TDTMA with
294 similar surface area of 8.8507 ~ 10.8419 m^2/g and the pore volume of 0.059 ~ 0.065 cm^3/g.
295 The organoclays at higher concentrations (1.0 ~ 2.0 CEC TDTMA) have the lower BET
296 surface area and pore volume, whereas montmorillonite has a largest BET surface area and
297 pore volume. From the result, it is assumed that the pore volume and surface area are not a
298 key factor in terms of control the affinity between organoclays and organic pollutants[16].
299 Hence, the loaded surfactant is highly important to determine the sorption mechanism onto
300 organoclays.

301

302

X-ray photoelectron spectroscopy (XPS)

X-ray photoelectron spectroscopy (XPS) is used to further determine the surface chemical composition and chemical states of prepared materials. This technique has been widely applied for the investigation of top few layers of material surface with partially filled valance band. Figure 7 shows the XPS survey scans of montmorillonite, surfactant (TDTMA), and representative organoclays (0.5 CEC-TDTMA and 2.0 CEC-TDTMA). The survey scan has an obvious verification in the presence of sodium, silicon, aluminium, iron, and magnesium in the montmorillonite. It has also indentified the presence of carbon, nitrogen, and bromine in TDTMA. A minor amount of carbon in montmorillonite and oxygen in TDTMA is observed as a result of adsorbed CO_2 [17]. The peaks of magnesium and iron (trace amount) are seen in the scans of organoclays, whereas the sodium peak is disappeared. Both magnesium and iron are located in the montmorillonite structure rather than in the interlayer. The absence of sodium ions in the organoclays confirms the sodium ions are exchanged when cationic surfactants are introduced in the interlayer. The prominent peaks of carbon and silicon are recorded in the montmorillonite and organoclays, the ratio of C/Si has been found and the ratio increased in the following order: 0.34 (montmorillonite) < 1.58 (0.5 CEC-TDTMA) < 1.70 (1.0 CEC-TDTMA) < 1.82 (1.5 CEC-TDTMA) < 2.55 (2.0 CEC-TDTMA). The intercalation of surfactant increases with an increased loading. Meanwhile, the Al/Si ratio dropped from 0.42 (montmorillonite) to 0.35 (1.0 CEC-TDTMA) and further 0.34 (2.0 CEC-TDTMA). As the intercalation of surfactants increases in the interlayer, the distance between Al-O(OH) octahedral sheets and two Si-O tetrahedral sheets in the structure of montmorillonite is expanded, and hence, the detecting ratio of Al and Si is lower. This is further investigated by the high-resolution XPS scans.

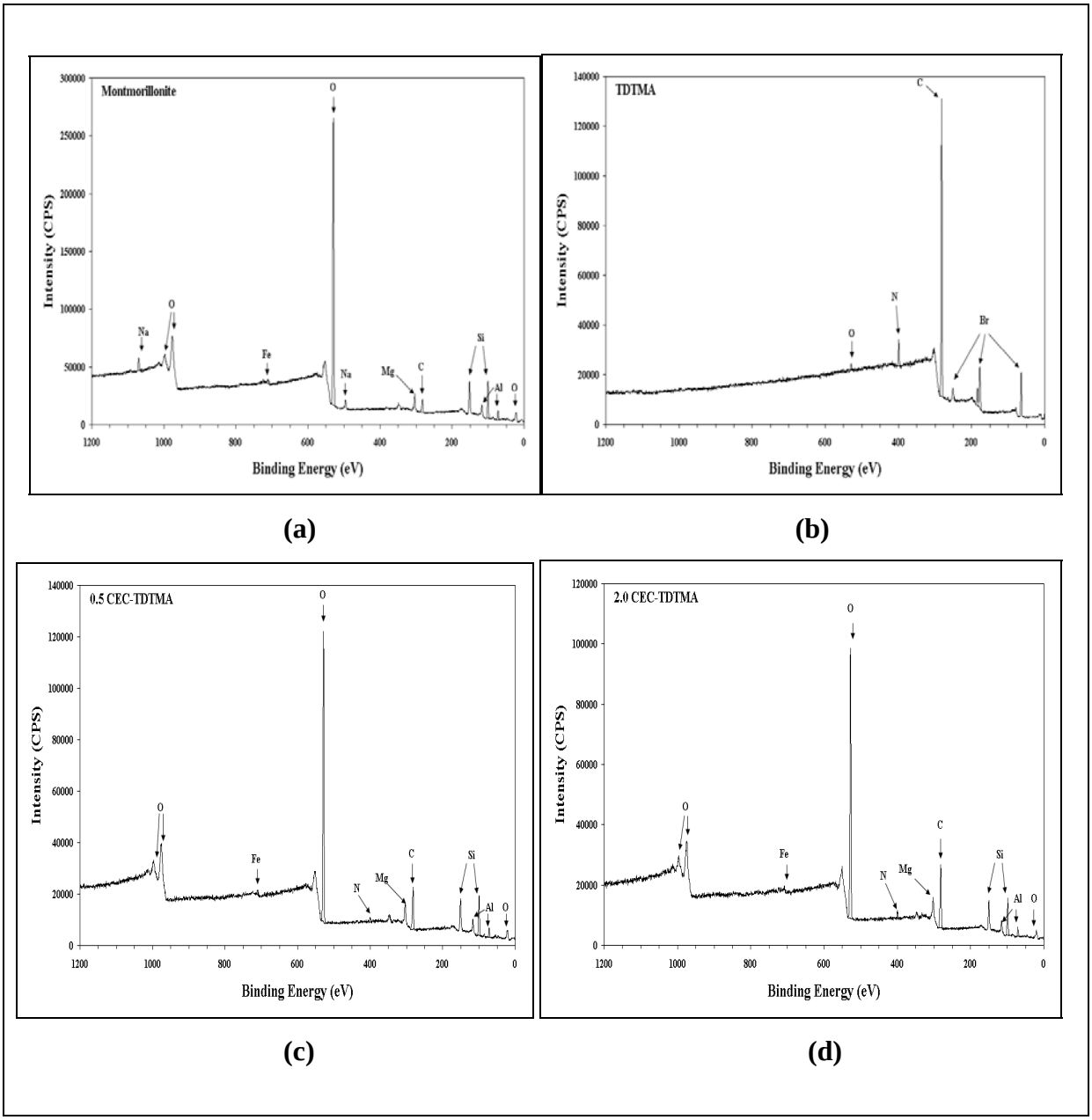

Figure 7. XPS survey scan spectra of montmorillonite (a), surfactant (b), and organoclays (c and d)

The high resolution XPS spectra of O 1s of montmorillonite and organoclays are compared in Figure 8. It hardly distinguishes between O and OH in the montmorillonite. The intense main peak with the binding energy of 529.42 eV corresponds to O(OH) in the montmorillonite structure, while the other small peak at 531.17 eV is considered as oxygen in H_2O. The small trace of an oxygen peak is not observed in organoclays due to their hydrophobic characteristics and the binding energy has decreased from 528.64 to 527.59 eV

when the surfactant loading increased from 0.5 to 2.0 CEC. This reduced binding energy is also observed in the high resolution Si 2p and Al 2p spectra (Figure 9). The decreased binding energy of both O 1s and Si 2p shows the change of interlayer structure in organoclays.

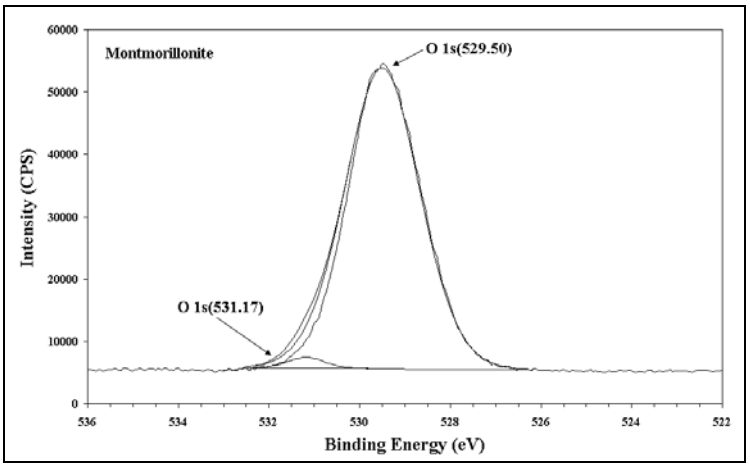

(a)

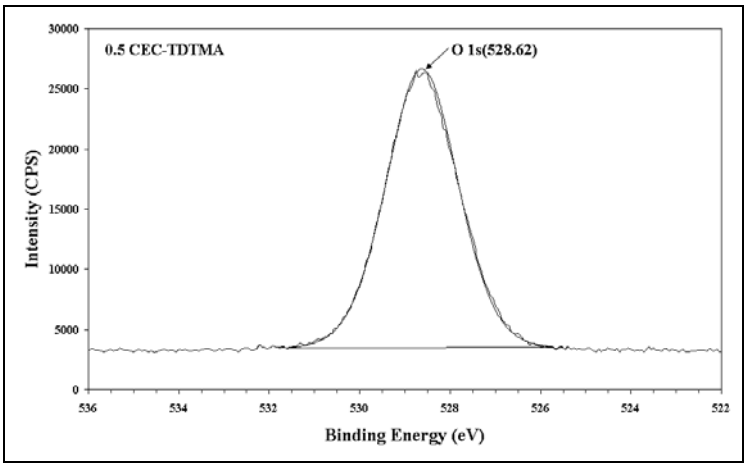

(b)

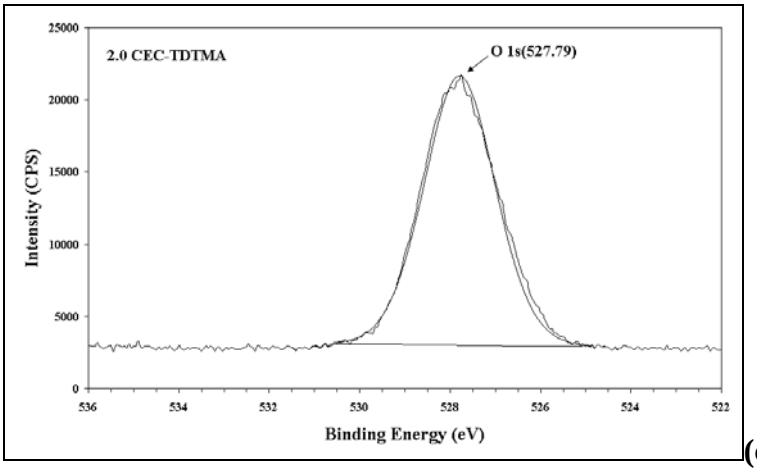

(c)

Figure 8. XPS high resolution spectra of O 1s for montmorillonite (a), organoclays (b, c)

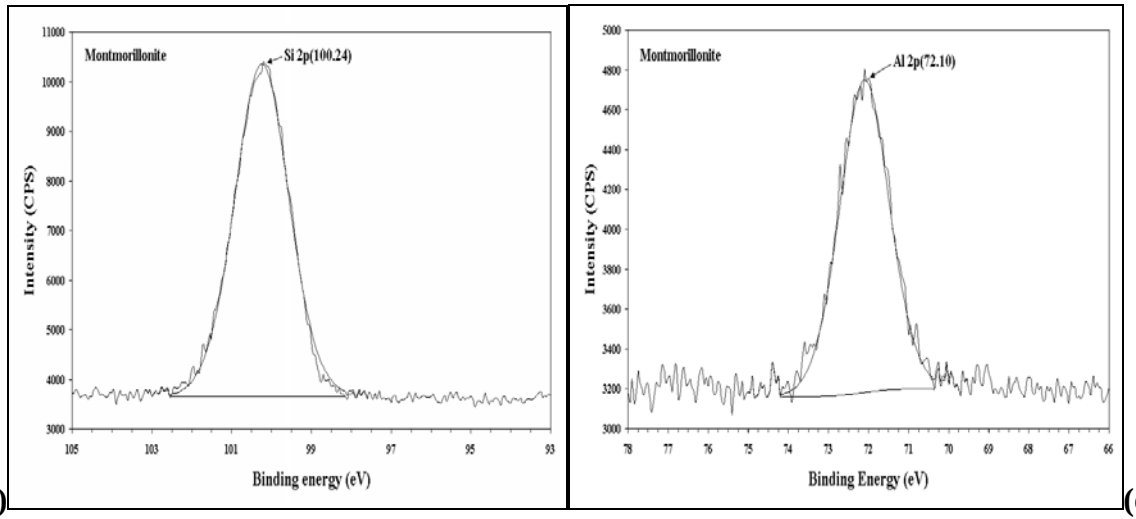

(a) (d)

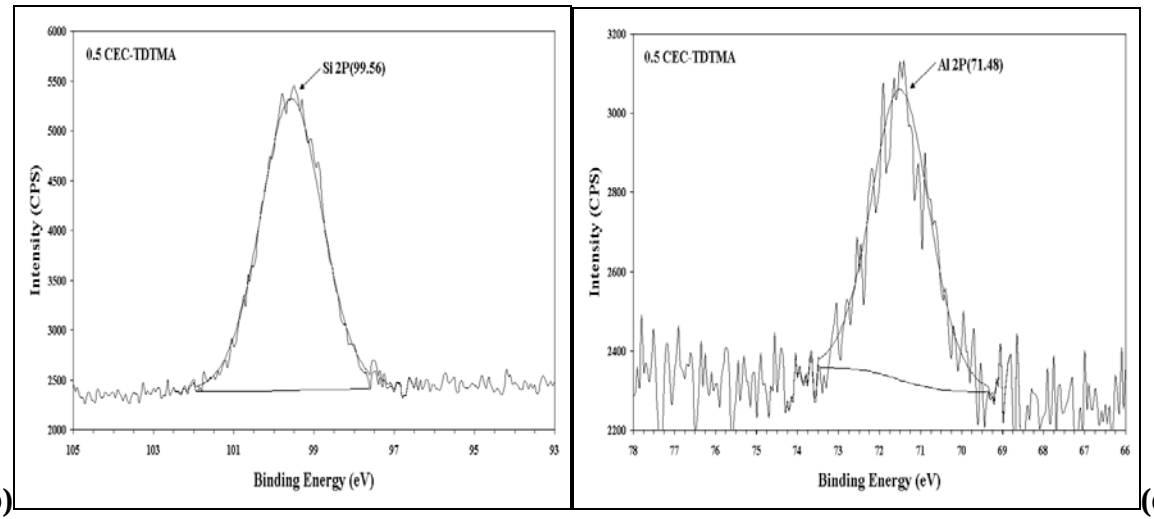

(b) (e)

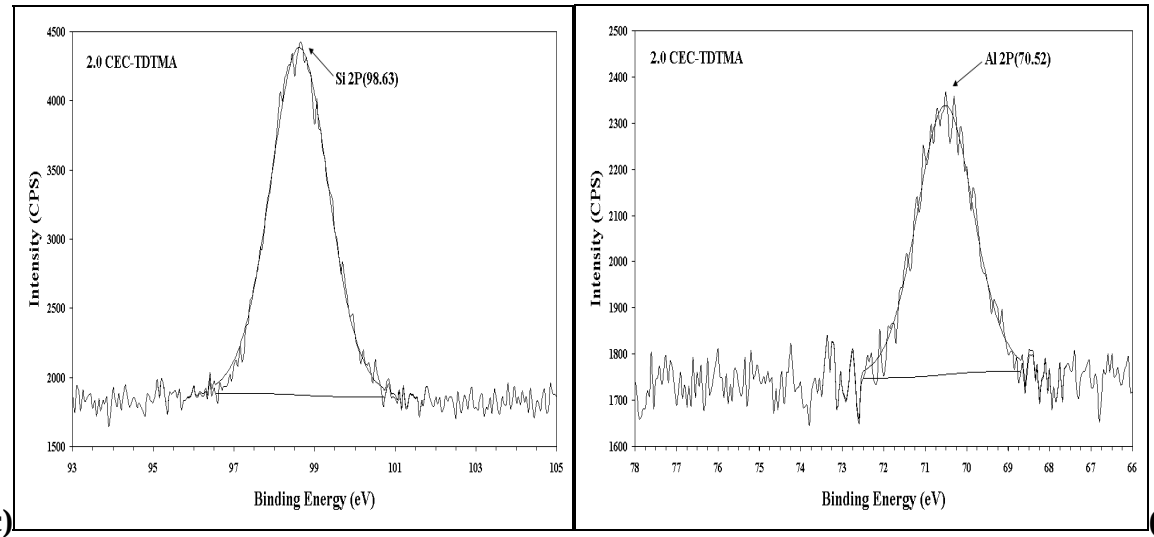

(c) (f)

Figure 9. XPS high resolution spectra of Si 2p and Al 2p for montmorillonite (a and d), organoclays (b, e and c, f)

In the high-resolution XPS spectra, C 1s of organoclays is characterised by two transitions at 281and 283 eV (Figure 10). The transition peak at about 281 eV is ascribed to the C-C bond in the long chain of the surfactant, and the C-N bond has a binding energy of about 283 eV. Table 2 shows the results for curve fitted binding energy and their atomic contents (at. %) of the highly resolved C 1s XPS spectra present in Figure 10. The binding energy for C-C bond increases gradually as the surfactant loading increases from 0.25 to 2.0 CEC in organoclays, while C 1s binding energy of C-N bonds remain similar. The result of C 1s binding energy for C-C bond shows that the loading surfactant affects the C 1s binding energy in organoclays. When the cationic surfactant is intercalated in the interlayer structure, the nitrogen as a head group in the alkyl surfactant interacts with the negative clay due to the electrostatic interaction. From the interaction between nitrogen head group and negative clay surface, the binding energy for C-N remains similar and the binding energy is not changed with an increase of the loading surfactant. However, the increasing binding energy for C-C bond may be explained by the arrangement of surfactant in the interlayer. At the lower concentration of the surfactant, the alkyl chains are parallel to the silica clay surface within the interlayer (e.g. monolayer or bilayer). As a result of an increase amount of loading surfactant, the arrangement of surfactant is at right angle to the clay mineral surface such as pseudo-trilayer or paraffin structures, which can be described using XRD. The increased packing density within the interlayer causes the increase of C-C binding energy in the alkyl chain.

Table 2 Binding energy and their atomic contents of C 1s for organoclays

C 1s (eV)	0.25 CEC	0.5 CEC	1.0 CEC	1.5 CEC	2.0 CEC
C-C bond	281.28 (74.91)	281.34 (72.83)	281.33 (76.09)	281.34 (77.55)	281.38(84.31)
C-N bond	283.08 (25.09)	283.09 (27.17)	283.04 (23.91)	283.08 (22.45)	283.09 (15.69)

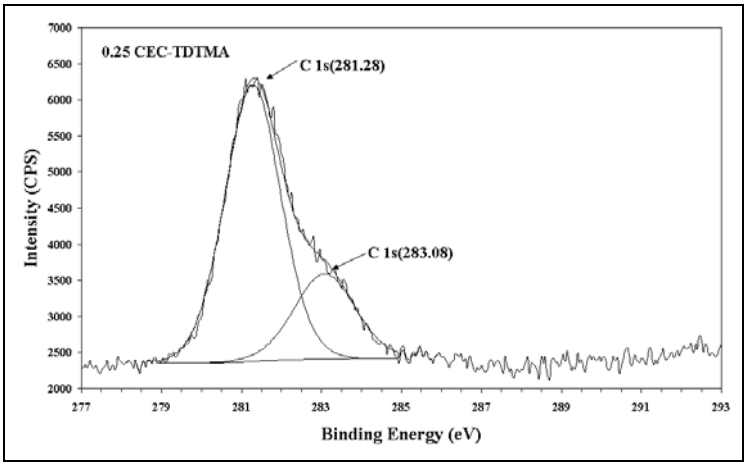

(a)

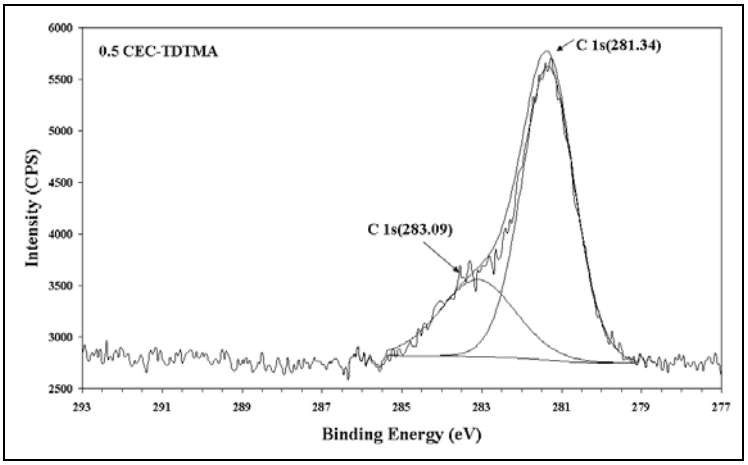

(b)

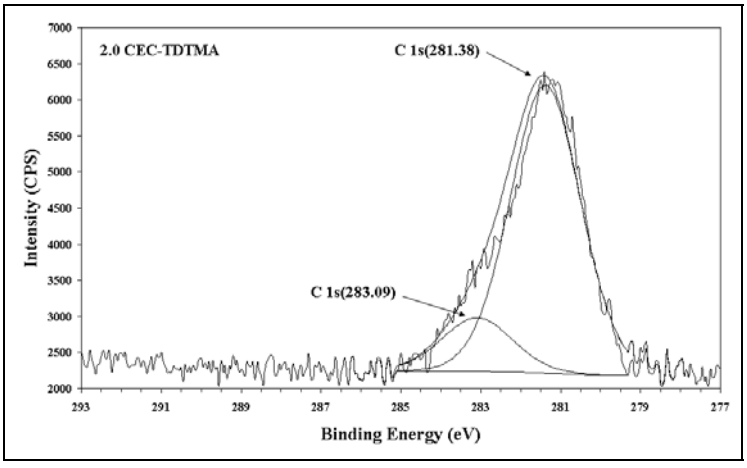

(c)

Figure 10. XPS high resolution spectra of C 1s for organoclays (a, b, c)

Bromine peaks were observed from the scan of the organoclays. However, the highly well resolved Br peaks are poorly obtained (not shown) and the content of bromine in organoclays is limited. The result indicates that the preparation of organoclays, which are free of Br ions

was successful and that the surfactant $TDTMA^+$ was highly exchanged with Na^+ within the interlayer [18, 19].

Thermogravimetric analysis (TGA)

Thermal stability of organoclays and packing arrangement of organic cationic surfactant within the organoclays at an elevated temperature were determined by TGA [4, 20, 21]. The TG and DTG curves for montmorillonite and the organoclays with and without p-nitrophenol are shown in Figures 11 and 12.

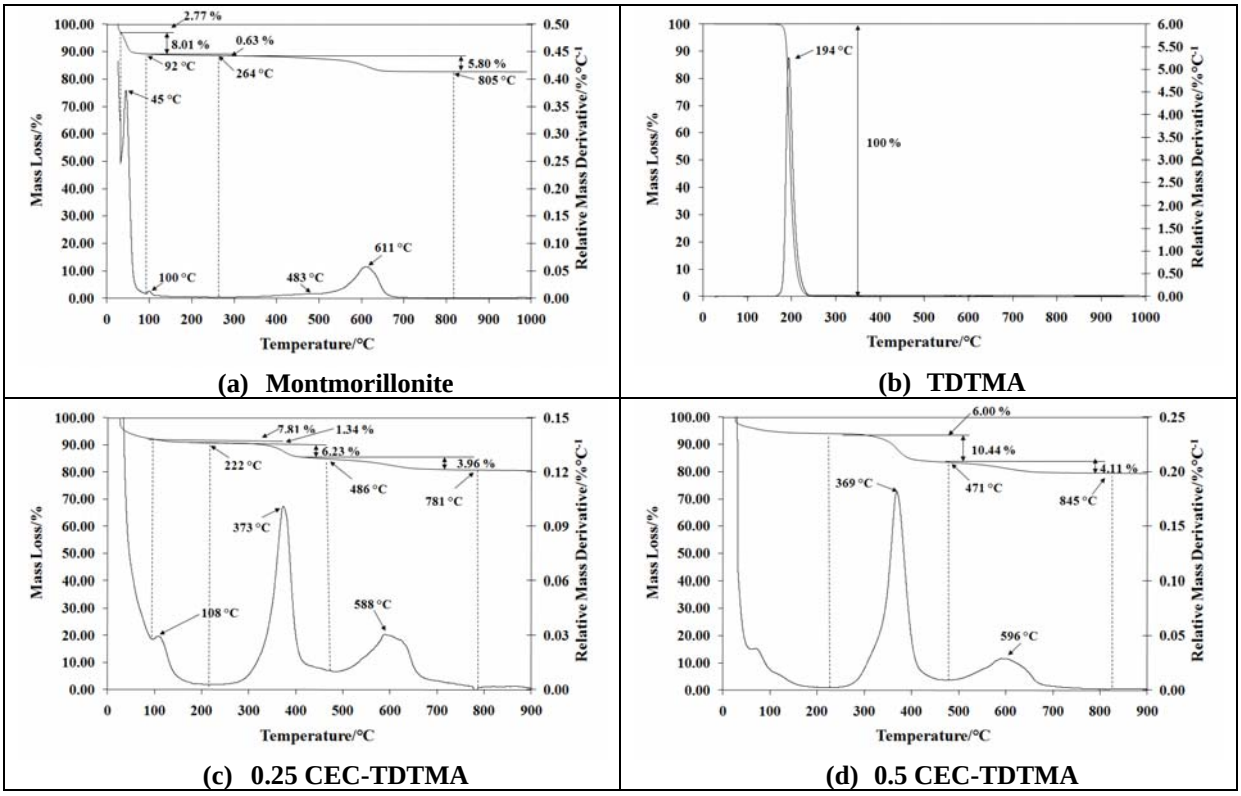

(a) Montmorillonite **(b) TDTMA**

(c) 0.25 CEC-TDTMA **(d) 0.5 CEC-TDTMA**

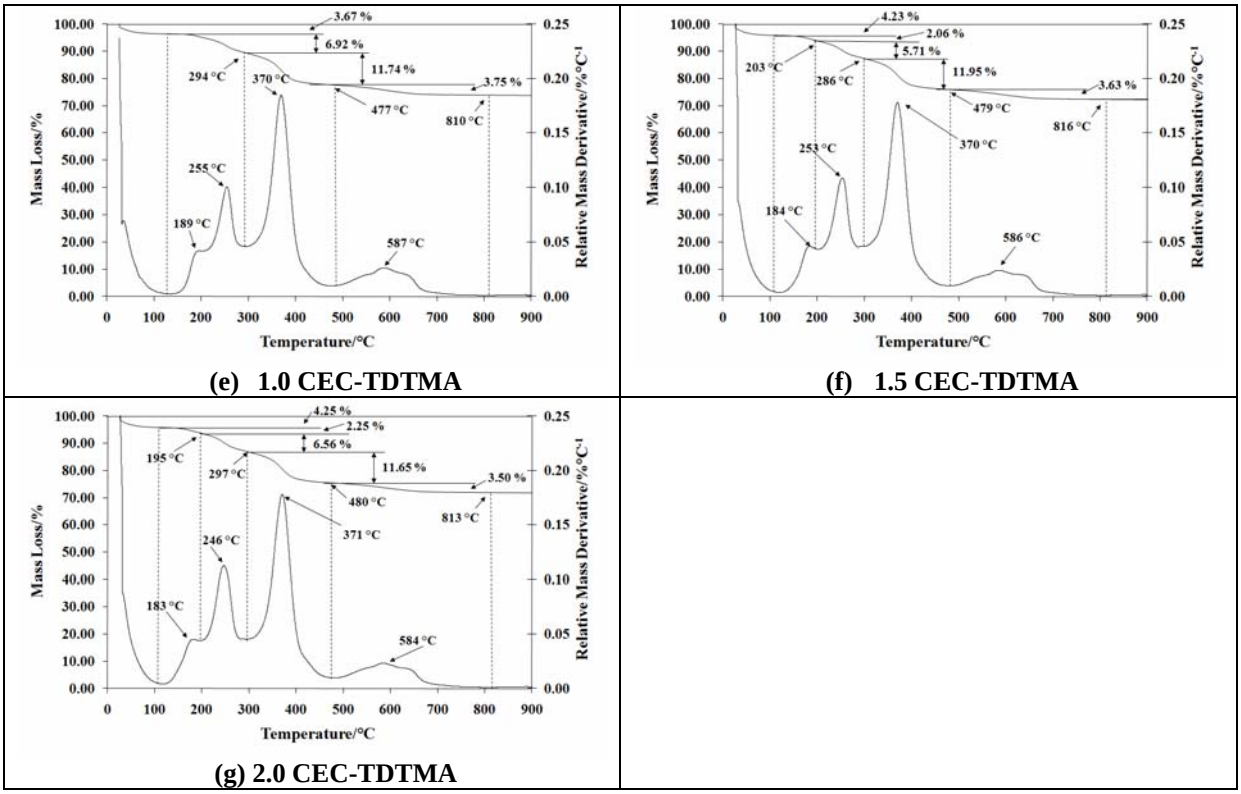

Figure 11.Thermogravimetric analyses of montmorillonite, Surfactant (TDTMA) and organoclays

In Figure 11, there are several mass loss steps observed. The first two mass loss steps of montmorillonite involve dehydration and/or dehydroxylation from room temperature and before 110 °C. The two steps are attributed to the dehydration of adsorbed water, and water molecules around metal cations such as Na^{+} or Ca^{2+} in the exchangeable sites of montmorillonite. The experimental mass loss peak during the second hydration and hydroxylation of adsorption water appears only for untreated montmorillonite and 0.25 CEC-TDTMA. The montmorillonite (Figure 11(a)) shows two thermal decomposition steps at both 483 and 611 °C, which were caused by the dehydroxylation of the montmorillonite. The decomposition at a lower temperature 483 °C is assigned to the loss of OH units at the end of clay layers, while the temperature at 611 °C is contributed by dehydroxylation of clay. However, the thermal decomposition of montmorillonite with adsorbed p-nitrophenol is differently shown. Figure 12(a) shows that the decomposition at 287 °C is occurred and this may be assigned to the adsorbed p-nitrophenol on the montmorillonite. It is reported by Zhou and colleagues that p-nitrophenol sublimes at 131 °C [22]. The reason for obtaining higher

temperature than 131 °C may be chemical reactions between the adsorbed p-nitrophenol and clay surface of montmorillonite.

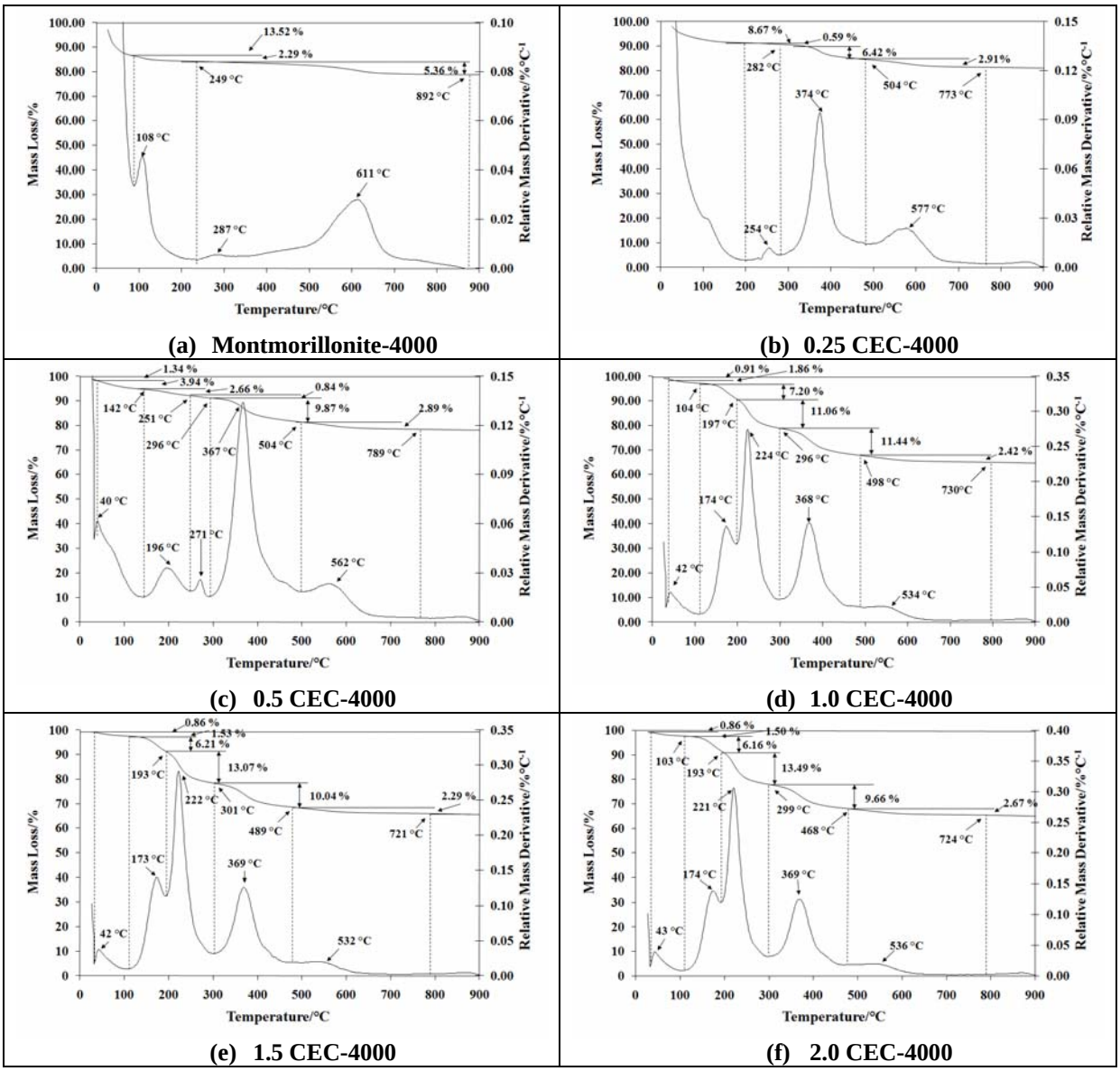

Figure 12. Thermogravimetric analyses of montmorillonite and organoclays adsorbed p-nitrophenol

One small dehydration peak for 0.25 CEC-TDTMA and 0.5 CEC –TDTMA is observed at 373 and 369 °C, respectively. Meanwhile, there are three peaks centred at 189/255/370 °C for 1.0 CEC-TDTMA, 184/253/370 °C for 1.5 CEC-TDTMA, and 183/246/371 °C for 2.0 CEC-

419 TDTMA. The third step is considered as the loss of surfactant by comparing the peak of pure
420 surfactant, which decomposes at 194 °C, with that of untreated montmorillonite. From the
421 results, it is proposed that the number of peaks in the third step is affected by the loading of
422 the surfactant. When the concentration of the organoclay is relatively low (e.g. 0.25 CEC and
423 0.5 CEC), there is a single peak observed (the peak position around 370 °C). The reason for
424 the single peak is that the organic cations exchange with Na^+ ions, which is mainly adhered to
425 the surface sites via electrostatic interactions [21]. With the increase of surfactant
426 concentration loading, some surfactant molecules tend to attach to the clay surface, which
427 results in the appearance of the second peak (the peak position around 250 °C). When the
428 surfactant loading has exceeded the CEC of the clay (1.0, 1.5, and 2.0 CEC), the surfactant
429 molecules strongly adhere to the clay surface by van der Waals forces, and this causes a new
430 peak to appear (at 183 ~ 185 °C). In addition, the intensity of the peaks increase with
431 increased surfactant loading. The effect causes the temperature of the decomposition
432 surfactant in the third step to increase. The second and third peaks for 1.0 CEC-TDTMA, 1.5
433 CEC-TDTMA, and 2.0 CEC-TDTMA compare closely to the pure surfactant peak at 194 °C,
434 and the temperature of the two peaks is gradually decreased.

435 The thermal decomposition peaks for organoclays with adsorbed p-nitrophenol are
436 observed in Figure 12. The two decomposition peaks of 0.25 CEC-4000 are observed at 254
437 and 374 °C. The formal is attributed to the adsorbed p-nitrophenol on organoclay, while the
438 later decomposition temperature is ascribed to the combustion of the surfactant. The thermal
439 decomposition of 0.5 CEC-4000 is very different from that of the organoclays. The main
440 difference is the presence of two peaks for the loss of adsorbed p-nitrophenol. Two thermal
441 decomposition steps at 196 and 271 °C are observed with mass losses of 2.66 and 0.84 % and
442 these may be formed from the result of the removal and desorption of p-nitrophenol in the
443 clay layers[22]. The mass loss at 367 °C of 9.87 % is the loss of the surfactant. When the
444 surfactant loading is increased above 0.5 CEC, three decomposition steps are observed for 1.0,
445 1.5, and 2.0 CEC adsorbed p-nitrophenol. The three decomposition temperatures are 174, 224,
446 and 368 °C for 1.0 CEC-4000, 173, 222, and 369 °C for 1.5 CEC-4000, and 174, 221, and
447 369 °C for 2.0 CEC-4000. The first two decomposition steps are assigned to the loss of
448 surfactant, and the later decomposition temperature is attributed to the loss of intercalated
449 surfactant molecules. The adsorbed p-nitrophenol peaks, which were found at 0.25 and 0.5
450 CEC, are not observed and this is assumed that the adsorbed p-nitrophenol is decomposed
451 simultaneously with the surfactant. During the desurfactant procedure, the experimental

452 mass loss increases from 6.23 % (0.25 CEC-TDTMA) to 20.46 % (2.0 CEC-TDTMA), and
453 100 % for the pure surfactant. The last mass loss over the temperature from 611 to 584 °C is
454 ascribed to the loss of hydroxylation from the structural inner OH units of the
455 montmorillonite. The dehydroxylation temperature in the organoclays upon the adsorption of
456 p-nitrophenol is lower because of the chemical reaction between adsorbed p-nitrophenol and
457 siloxane clay surfaces. The chemical binding of the p-nitrophenol to the inner OH units
458 reduces the dehydroxylation temperature. The intensity of the peak decreases with increase in
459 the surfactant concentrations.

460 **Table 3** TGA results of montmorillonite (MMT), surfactant (TTMAB), and organoclays with
461 and without adsorbed p-nitrophenol

Sample	**Dehydration/ hydroxylation**		**Dehydration/ dehydroxylation**		**Desurfactant**		**Dehydroxylation (OH unit)**	
	% mass loss **(step 1)**	Temp. (°C)	% mass loss **(step 2)**	Temp. (°C)	% mass loss **(step 3)**	Temp. (°C)	% mass loss **(step 4)**	Temp. (°C)
Montmorillonite	10.78	-	0.63	100	-	-	5.80	483,611
0.25 CEC-TDTMA	7.81	-	1.34	108	6.23	373	3.96	588
0.5 CEC-TDTMA	6.00	-	-	-	10.44	369	4.11	596
1.0 CEC-TDTMA	3.67	-	-	-	18.66	189, 255, 370	3.75	587
1.5 CEC-TDTMA	4.23	-	-	-	19.72	184, 253, 370	3.63	586
2.0 CEC-TDTMA	4.25	-	-	-	20.46	183, 246, 371	3.50	584
TTMAB	-	-	-	-	100	194	-	-
MMT-4000	13.52	-	2.29	108			5.36	611
0.25 CEC-4000	8.67	-	-	-	0.59[a],6.42	254[b],374	2.91	577
0.5 CEC-4000	5.28	-	-	-	13.37	196[b], 271[b], 367	2.89	562
1.0 CEC-4000	2.77	-	-	-	29.70[c]	(174, 224, 368)[d]	2.42	534
1.5 CEC-4000	2.39	-	-	-	29.32[c]	(173, 222, 369)[d]	2.29	532
2.0 CEC-4000	2.36	-	-	-	29.31[c]	(174, 221, 369)[d]	2.67	536

462 [a] Mass loss of adsorbed p-nitrophenol

463 [b] Thermal decomposition of adsorbed p-nitrophenol

464 [c] Mass loss of adsorbed p-nitrophenol and surfactant

465 [d] Thermal decomposition of adsorbed p-nitrophenol and surfactant

466

467 It is summarised that four steps are discernible from DTG figure (Figures 11 and 12, and
468 Table 3). The first two steps involve the dehydration and/or dehydroxylation of adsorbed
469 water and water adsorbed by the metal cations. The decomposition of the surfactant at the
470 temperature between 184 and 373 °C is observed in the third step. Upon the adsorption of p-
471 nitrophenol, the decomposition of adsorbed p-nitrophenol is determined and the organoclays
472 above 0.5 CEC, p-nitrophenol is decomposed simultaneously with the surfactant. In the last
473 step, the dehydroxylation of OH structural units in the clay is observed at the temperature
474 from 611 to 584 °C. It is noted that the temperatures for the loss of p-nitrophenol are
475 relatively greater than that for the pure p-nitrophenol, and this indicates the p-nitrophenol
476 molecules are strongly bonded to the organoclay, which leads to lower dehydroxylation
477 temperature.

478

479 **Fourier transform Infrared spectroscopy (FT-IR)**

480 Infrared spectroscopy is an essential method to probe the molecular environment of the
481 intercalated surfactant for the organoclays [23]. From the observed infrared spectra, there are
482 several distinct regions: OH stretching region (3700 ~ 3000 cm^{-1}), CH stretching region
483 (2900 ~ 2800 cm^{-1}), HOH bending vibration region (1700 ~ 1600 cm^{-1}) and HCH bending
484 vibration region (1520 ~ 1400 cm^{-1}).

485 (i) OH stretching region

486

487 As shown in Figure 13, the infrared spectrum of montmorillonite and organoclays
488 (a) and with adsorbed p-nitrophenol (b) in the OH stretching region is characterised
489 by two bands at 3700 ~ 3000 cm^{-1}.

490

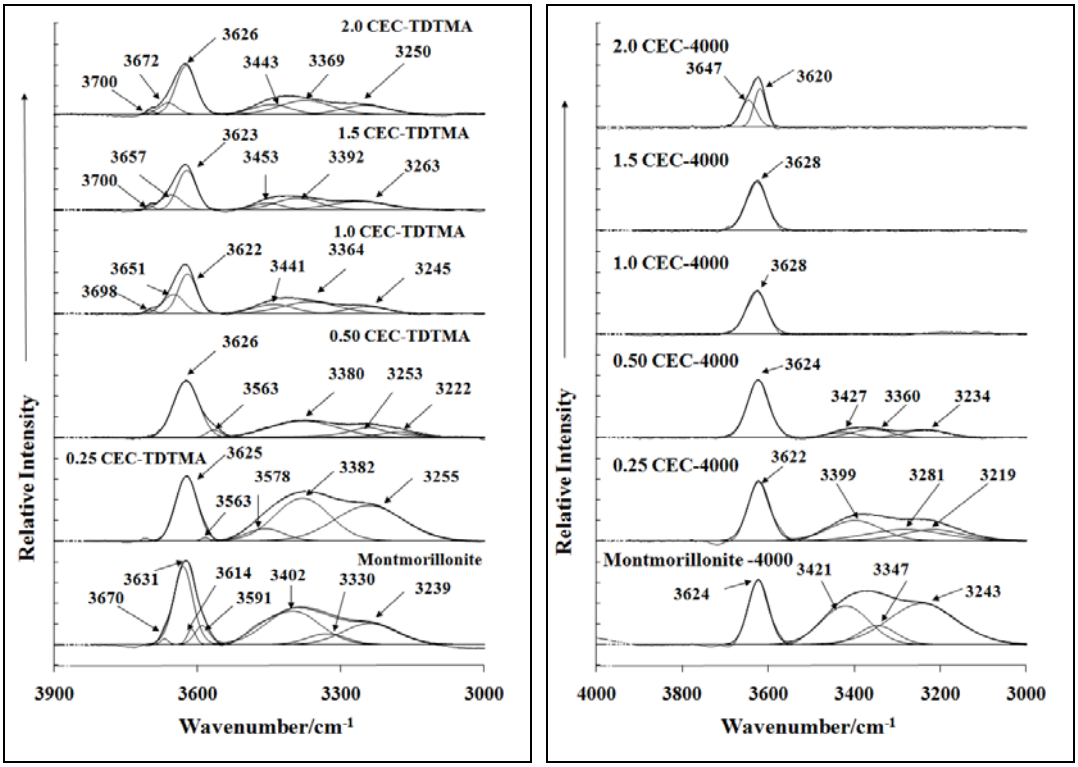

(a) (b)

Figure 13. Infrared spectroscopy of montmorillonite and organoclays with and without p-nitrophenol in 3900 ~ 3000 cm^{-1} spectral range

A sharp and intense peak at 3631cm^{-1} for montmorillonite is assigned to OH stretching vibrations of the structural hydroxyl group, while the broad bands at 3402, 3330, and 3230 cm^{-1} are ascribed to other water hydrogen bonded to water molecules adsorbed within the interlayer of the clay (see Figure 13a). The infrared spectrum of montmorillonite with adsorbed p-nitrophenol shows peaks in similar position to that of non-reacted montmorillonite (see Figure 13b). The bands at 3421, 3347, and 3243cm^{-1} for montmorilllonite-4000 shows an increased intensity than that of montmorillonite. However, the bands for water hydrogen bonded to other water molecules no longer existed when the surfactant loading has exceeded the CEC of the clay. This is in great agreement with the study by Zhou et. al. There is a hydrogen bond between p-nitrophenol with water for untreated montmorillonite and organoclays at low CEC concentrations [6].

The position of the sharp band corresponding to the OH vibrations of the structural hydroxyl groups is relatively independent of the surfactant concentration. However, the broad bands between 3500 ~ 3200 cm^{-1} are strongly dependent on the surfactant concentration loading. At low concentrations of surfactant, the infrared spectrum of 0.25 CEC-TDTMA showed the broad adsorption band near 3382 cm^{-1} with shoulders at 3578 and 3255 cm^{-1}. The band shifted to lower wavenumber from 3382 to 3364 cm^{-1} with an increase in the surfactant loading up to 1.0 CEC-S. The change in wavenumber is related to the environment of water. In addition, additional bands at 3672 and 3700 cm^{-1} are observed above 1.0 CEC-TDTMA and this is suggested that the water in the montmorillonite is gradually displaced with the surfactant (TDTMA), and that the surfactant is adsorbed on other surfactant molecules, which have already been adsorbed in the clay interlayer.

(ii) CH stretching region

The spectra of the CH stretching region for montmorillonite and organoclays at different surfactant loadings and with p-nitrophenol are shown in Figure 14. No bands attributable to the CH stretching vibrations were observed for montmorillonite and montmorillonite-4000. However, infrared bands in the region between 2700 and 2900 cm^{-1} are observed for organoclays modified with TDTMA, and these are ascribed to the asymmetric $\nu_{as}(CH_2)$ and symmetric $\nu_s(CH_2)$ stretching modes of the surfactant. It is observed that the CH_2 asymmetric stretching modes slightly shifted to lower wavenumbers upon intercalation of the surfactant molecules (from 2927 to 2925 cm^{-1}). The wavenumber of the symmetric CH_2 stretching modes is shifted to 2848 cm^{-1} from 2853 cm^{-1}. From the spectra, the wavenumbers of the asymmetric and symmetric CH stretching modes of amine chains in the region indicated the conformational difference between organoclays intercalated with TDTMA at the various CEC concentrations. Li and Ishida [24] reported that the chains are highly ordered (all-trans conformation), the wavenumbers are decreased with in accordance to the increase of ordered conformers within the clay interlayers. Similarly, the asymmetric and symmetric CH stretching modes shifted to low wavenumbers for organoclays adsorbed with p-nitrophenol. It is suggested that these two CH stretching peaks are extremely sensitive to the conformational changes of the chain within the interlayer, where the wavenumber decreases as the loading of the

surfactant increase from 0.25 to 2.0 CEC. Similar results have been shown in some previous studies [25, 26]. Thus the wavenumbers of the CH stretching bands are highly sensitive to the conformational changes of the chain, which can be qualitatively monitored by the wavenumber shifts. In addition, a significant wavenumber shift indicates more gauche conformational molecules introduced into alkyl chain with the decrease of alkyl chain length. The conformation of adsorbed long alkyl chain surfactants progressively forms a solid like molecular environment (with high packing density and ordering), and this increase in surfactant packing density can lead to the expansion of clay mineral interlayer spaces, which can be characterised by XRD.

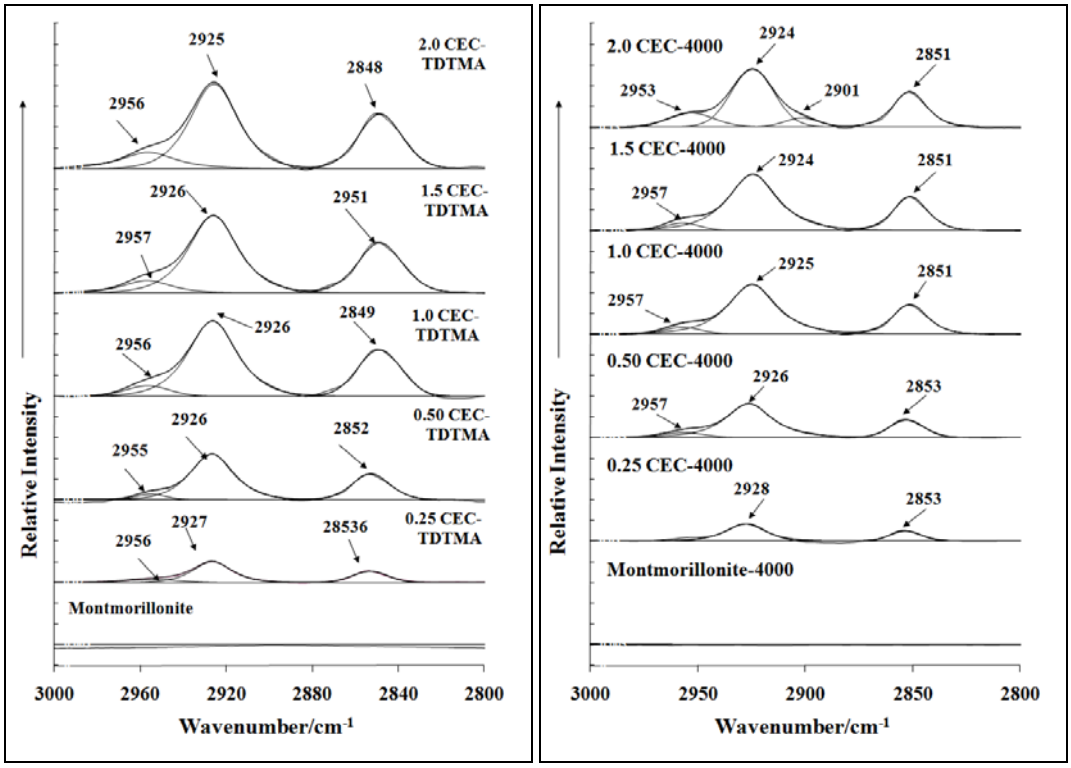

(a) (b)

Figure 14. Infrared spectroscopy of montmorillonite and organoclays with and without p-nitrophenol in the 3000 ~ 2800 cm^{-1} spectral range

(iii) HOH and HCH bending vibrations

Figure 15a presents the changes in the adsorption bands related to the HOH bending vibrations of the water molecules adsorbed on montmorillonite and organoclays.

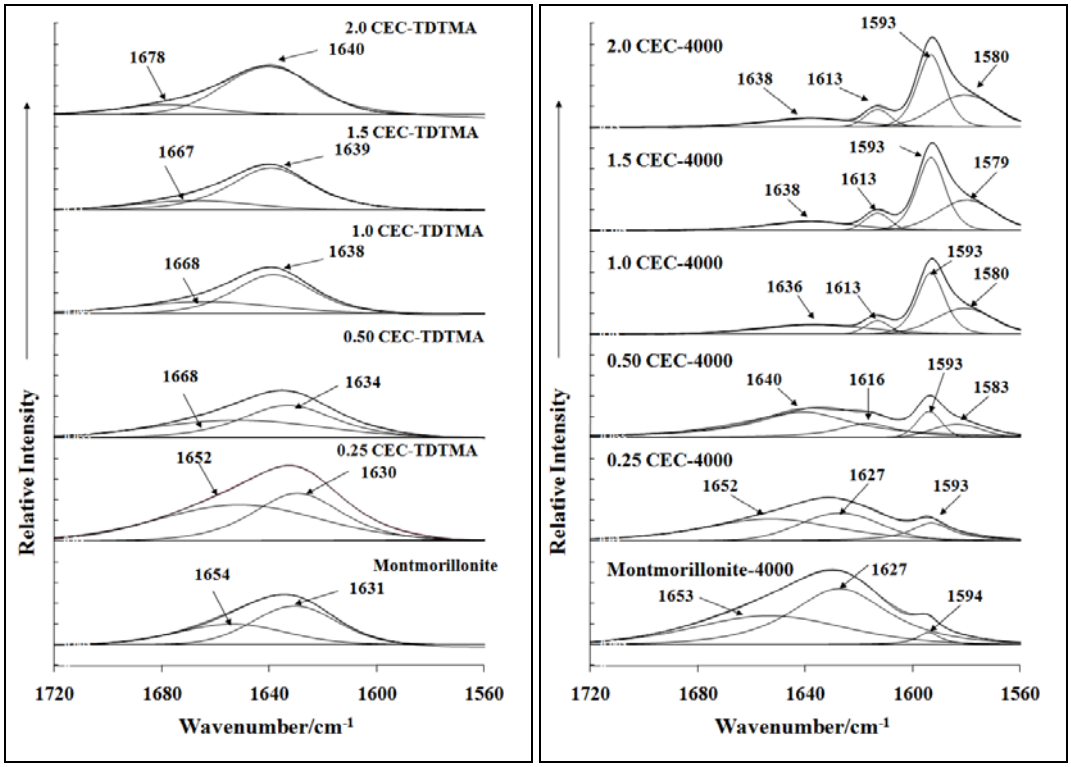

(a) (b)

Figure 15. Infrared spectroscopy of montmorillonite and organoclays with and without p-nitrophenol in the 1720 ~ 1560 cm^{-1} spectral range

The positions at these bands for montmorillonite are at 1631 cm^{-1} with a shoulder at 1654 cm^{-1}. It is apparent from Figure that the wavenumber of the water bending peaks shifted significantly to higher wavenumbers from 1630 cm^{-1} with the increase in surfactant concentration. However, the intensity of this adsorption band decreased, and this can be attributed to the amount of hydrogen bonded water molecules at the high surfactant concentration level (for example, 2.0 CEC-TDTMA) is less than that at lower surfactant concentrations (for example, 0.25 CEC-TDTMA).

The IR spectra of montmorillonite and organoclays with adsorbed p-nitrophenol are shown in Figure 15b. The HOH bending modes for montmorilonite-4000 are observed at 1627 cm^{-1} with a shoulder of 1653 cm^{-1}. An additional small peak at 1594 cm^{-1} appears, and this is assigned to adsorbed p-nitrophenol compared to the spectra of non-reacted montmorillonite. From the literature[6], the peak at 1599 cm^{-1} is ascribe to C=C aromatic stretching vibration, and the OH deformation modes of p-nitrophenol is present at 1623 cm^{-1}.The wavenumber of OH bending peaks of organoclays with adsorbed p-nitrophenol are gradually shifted from 1627 cm^{-1} to 1613 cm^{-1} with an increase of loading surfactant. The intensity of the water bending modes is gradually decreased with the increase of surfactant loading, whereas the intensity of p-nitrophenol at 1594 cm^{-1} is significantly increased. It is proposed that p-nitrophenol is highly reacted with clay surface in the organoclays, and that as a result of the intercalation of the surfactant, the surface property of montmorillonite is modified from hydrophilic to hydrophobic.

Major peaks in the region between 1360 and 1560 cm^{-1} appeared to be due to the methylene scissoring modes and the HCH deformation region of the TDTMA intercalated montmorillonite as shown in Figure 16a.

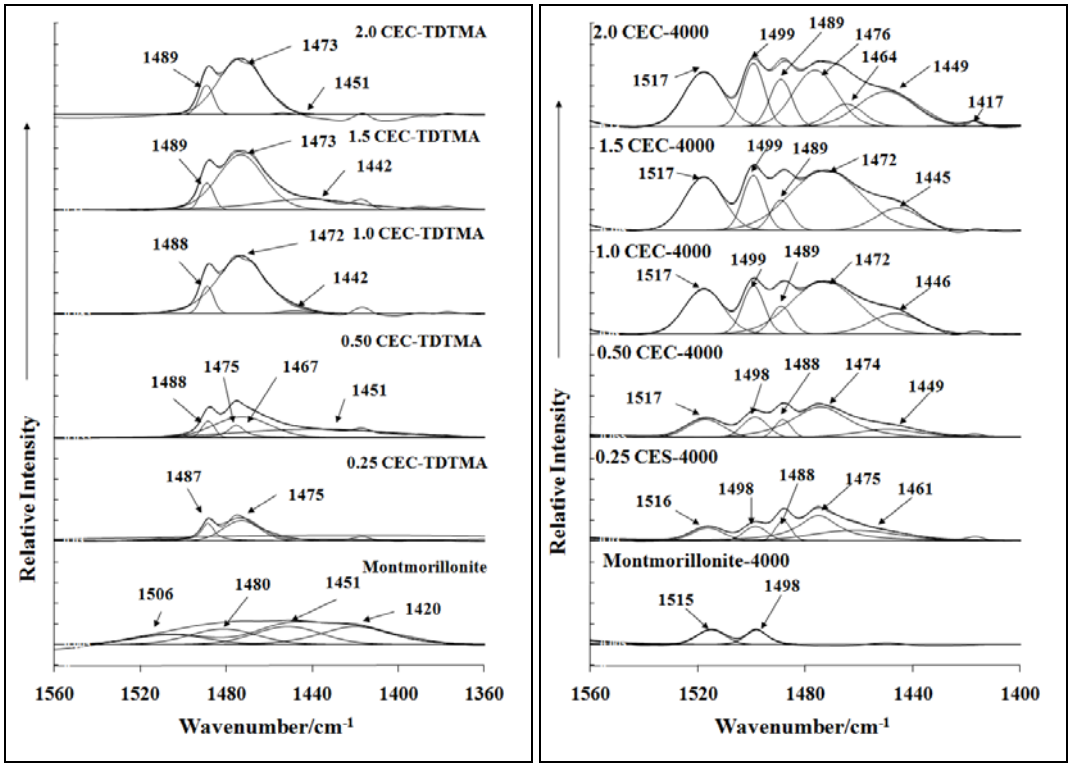

(a) (b)

Figure 16. Infrared spectroscopy of montmorillonite and organoclays without p-nitrophenol in the 1560 ~ 1360 cm^{-1} spectral range

The bands in this region for montmorillonite are found at 1506, 1480, 1451, and 1420 cm^{-1}. However, the band at 1506 and 1420 cm^{-1} are not observed in the surfactant intercalated with montmorillonite. At low CEC surfactant concentration (0.25 CEC-TDTMA), two small peaks at 1487 and 1475 cm^{-1} appeared and the intensity of these peaks increases with increase in the surfactant loading. The IR spectra of montmorillonite and organoclays with adsorbed p-nitrophenol are shown in Figure 16b. The peak at 1515 cm^{-1} in montmorillonite is drawn by the adsorbed p-nitroophenol as antisymmetric NO_2 stretching vibrations (at 1523 cm^{-1}). The wavenumber from 1523cm^{-1} to 1515 cm^{-1} provides again a strong evidence for the reaction between p-nitrophenol with the montmorillonite clay surfaces. The intensity of peaks at 1498, 1488, 1475, and 1461 cm^{-1} increases with increase in the surfactant loading.

Adsorption of p-nitrophenol on organoclays

The prepared montmorillonite and organoclays are used for the adsorption study of p-nitrophenol in water, and the results are given in Figure 17. The adsorbed amounts of p-nitrophenol onto montmorillonite and organoclays increase in order: montmorillonite < 0.25 CEC-TDTMA<0.5 CEC-TDTMA<1.0 CEC-TDTMA<1.5 CEC-TDTMA<2.0 CEC-TDTMA. The amount of adsorbed p-nitrophenol on organoclays is larger than that on montmorillonite. It is also found that the addition of surfactants is in organoclays would increase the amount of adsorbed p-nitrophenol on organoclays. Therefore, the amount of loaded surfactant is important factor to determine the adsorbed amount of p-nitrophenol onto organoclays.

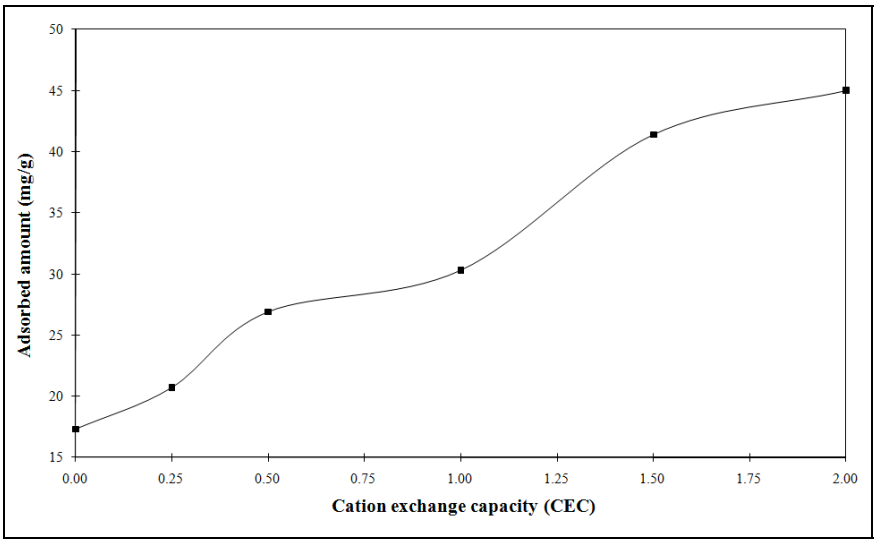

Figure 17. Uptake of p-nitrophenol on montmorillonite and organoclays

From the characterisation studies of montmorillonite and organoclays, the mechanisms of adsorbed p-nitrophenol are suggested. Montmorillonite has mainly electrostatic attraction between p-nitrophenol and hydrated cations in interlayer space of the clay and therefore, the larger d-spacing is observed in XRD pattern [27]. As the loaded surfactant molecules in the interlayer space of clay, the surface properties for organoclays convert from hydrophilic to hydrophobic and the intercalated surfactant molecules are also sorbed outside the clay layer. From the study of BET, there are two groups of organoclays observed. For organoclays prepared at relatively low surfactant loadings (0.25 and 0.5 CEC), surfactant molecules are preferred to intercalated in the interlayer space of clays, hence, p-nitrophenol molecules have

adsorbed in the interlayer space of organoclays and the organoclays intercalated with surfactant molecules are an excellent medium for partition of p-nitrophenol [28]. However, organoclays prepared at surfactant loadings exceed 1.0 CEC, surfactant molecules are highly intercalated in the clay interlayer space as well as interparticle pores, which lead to decreased surface area and pore volume. Hence, the clay layers are almost completely enclosed, and the pores are enlarged by the loaded surfactant molecules. The p-nitrophenol molecules can be captured not only within the clay layer space but also in the enlarged pores. The organoclay as a partition medium has strong affinity on p-nitrophenol molecules [29] and its efficiency is shown in the adsorption curves in Figure 17.

Accordingly, the sorption efficiency of the corresponding organoclays is higher than montmorillonite. Based on the distribution and arrangement of surfactant in organoclays, the mechanism is suggested as: the sorption mechanism of organic molecules at the organoclays (1.0 CEC ~ 2.0 CEC) is controlled by partition, whereas the organoclays prepared at lower surfactant loadings are mainly adsorption [7, 30-32].

Conclusions

Organoclays were prepared using montmorillonite and tetradecyltrimethylammonium bromide (TDTMA) as an example of a surfactant with a long alkyl chain. The prepared organoclays were characterised by modern physical techniques. Based on the basal spacing from the XRD pattern, information of the molecular arrangement within the clay interlayer space has been obtained as a function of the surfactant concentration. The configurations of the surfactant within the organoclays take a lateral monolayer arrangement at lower surfactant concentration (0.25 and 0.5 CEC). At higher surfactant concentrations (1.0 ~ 2.0 CEC), both configurations of the surfactant (a lateral bilayer and pseudotrimolecular layer structures) were observed. Moreover, the XRD pattern of organoclays adsorbed p-nitrophenol indicated the intercalation of p-nitrophenol within organoclays, and the expanded interlayer spacing of organoclays were measured and identified using TEM. Using BET method, it is found that the surface area is inversely related to the pore volume for organoclays. As the loading of the surfactant increase in organoclays, the pore size becomes smaller with an increase of surface area. Hence, it is concluded that the pore parameters are significantly related to the distribution and arrangement of surfactant intercalated into the clay surface. The loaded surfactant in the interlayer space were further analysed by TGA. Throughout the XPS study,

685 the chemical composition of montmorillonite and organoclays were analysed and the binding
686 energy of C-C is relatively sensitive to determine the structural changes in organoclays. In
687 infrared spectra, the CH stretching region was extremely sensitive to conformation changes
688 of the chain within the interlayer and a significant wavenumber shift indicates that more
689 gauche conformational molecules introduced into alkyl chain with the decrease of alkyl chain
690 length. From the results, the structural properties of organoclays intercalated with surfactant
691 were changed from hydrophilic to hydrophobic, and the adsorbed p-nitrophenol intercalates
692 the organoclay and displaces the surfactant molecules or rearranges the structure of surfactant
693 molecules within the organoclay interlayer. In addition, the different sorption mechanisms
694 involving adsorption and/or partition may affect the sorption of p-nitrophenol onto
695 organoclays. This type of organoclays will potentially be used as good adsorbents for
696 recalcitrant organic molecules in the industry and this organoclay will be applied to test in
697 adsorbing efficiency from p-nitrophenol and further removal of herbicides and pesticides
698 from contaminated samples.

699

700 **Acknowledgment**

701 Authors gratefully acknowledge and express gratitude to Dr. Barry Wood from the XPS
702 facilities at University of Queensland for his assistance and availability. We also would like
703 to thank Jin Cheng for his assistance with the TEM analysis.

704

705

706

707

708

709

710

711

712

References

[1] J.A. Smith, P.R. Jaffe, C.T. Chiou, Environmental Science & Technology 24 (1990) 1167.

[2] L.B. de Paiva, A.R. Morales, F.R. Valenzuela Díaz, Applied Clay Science 42 (2008) 8.

[3] M.O. Adebajo, R.L. Frost, J.T. Kloprogge, O. Carmody, S. Kokot, Journal of Porous Materials 10 (2003) 159.

[4] Y. Xi, R.L. Frost, H. He, T. Kloprogge, T. Bostrom, Langmuir 21 (2005) 8675.

[5] H. He, J. Duchet, J. Galy, J.-F. Gérard, Journal of Colloid and Interface Science 295 (2006) 202.

[6] Q. Zhou, R.L. Frost, H. He, Y. Xi, M. Zbik, Journal of Colloid and Interface Science 311 (2007) 24.

[7] M. Cruz-Guzman, R. Celis, M.C. Hermosin, W.C. Koskinen, J. Cornejo, Journal of Agricultural and Food Chemistry 53 (2005) 7502.

[8] G. Yuan, Journal of Environmental Science and Health, Part A: Toxic/Hazardous Substances and Environmental Engineering 39 (2005) 2661

[9] L. Zhu, B. Chen, X. Shen, Environmental Science & Technology 34 (1999) 468.

[10] Y. Xi, M. Mallavarapu, R. Naidu, Applied Clay Science 48 (2010) 92.

[11] R. Liu, R.L. Frost, W.N. Martens, Y. Yuan, Journal of Colloid and Interface Science 327 (2008) 287.

[12] S. Brunauer, L.S. Deming, W.E. Deming, E. Teller, Journal of the American Chemical Society 62 (1940) 1723.

[13] S.J. Gregg, K.S.W. Sing, Adsorption, Surface Area and Porosity. Academic Press, London and New York, 1967.

[14] M.A. Vicente, M. Suárez, J.d.D. López-González, M.A. Bañares-Muñoz, Langmuir 12 (1996) 566.

[15] C.-C. Wang, L.-C. Juang, C.-K. Lee, T.-C. Hsu, J.-F. Lee, H.-P. Chao, Journal of Colloid and Interface Science 280 (2004) 27.

[16] H. He, Q. Zhou, W.N. Martens, T.J. Kloprogge, P. Yuan, Y. Xi, J. Zhu, R.L. Frost, Clays and Clay Minerals 54 (2006) 689.

[17] L. Bugyi, A. Oszkó, F. Solymosi, Surface Science 461 (2000) 177.

[18] H. He, Q. Zhou, R.L. Frost, B.J. Wood, L.V. Duong, J.T. Kloprogge, Spectrochimica Acta Part A: Molecular and Biomolecular Spectroscopy 66 (2007) 1180.

[19] Z. Klapyta, T. Fujita, N. Iyi, Applied Clay Science 19 (2001) 5.

[20] H. He, Z. Ding, J. Zhu, P. Yuan, Y. Xi, D. Yang, R.L. Frost, Clays and Clay Minerals 53 (2005) 287.

[21] Y. Xi, Q. Zhou, R.L. Frost, H. He, Journal of Colloid and Interface Science 311 (2007) 347.

[22] Q. Zhou, H. He, R.L. Frost, Y. Xi, The Journal of Physical Chemistry C 111 (2007) 7487.

[23] J. Zhu, H. He, L. Zhu, X. Wen, F. Deng, Journal of Colloid and Interface Science 286 (2005) 239.

[24] Y. Li, H. Ishida, Langmuir 19 (2003) 2479.

[25] Y. Ma, J. Zhu, H. He, P. Yuan, W. Shen, D. Liu, Spectrochimica Acta Part A: Molecular and Biomolecular Spectroscopy 76 (2010) 122.

[26] R. Zhu, L. Zhu, J. Zhu, L. Xu, Applied Clay Science 42 (2008) 224.

[27] Q. Zhou, H.P. He, J.X. Zhu, W. Shen, R.L. Frost, P. Yuan, Journal of Hazardous Materials 154 (2008) 1025.

[28] H. He, Q. Zhou, W.N. Martens, T.J. Kloprogge, P. Yuan, Y. Xi, J. Zhu, R.L. Frost, Clays and Clay Minerals 54 (2006) 689.

762 [29] S.A.M. Boyd, M.M.; Chiou, C.T., Soil Science Society of America journal 52 (1988)
763 652.
764 [30] M. Cruz-Guzmán, R. Celis, M.C. Hermosín, J. Cornejo, Environmental Science &
765 Technology 38 (2003) 180.
766 [31] J.-F. Lee, M.M. Mortland, C.T. Chiou, D.E. Kile, S.A. Boyd, Clays and Clay
767 Minerals 38 (1990) 113.
768 [32] W.F.M.S.U. Jaynes, East Lansing, MI); Boyd, S.A., Soil Science Society of America
769 journal 55 (1991) 43.
770
771
772
773
774
775
776
777
778
779
780
781
782
783
784
785
786
787
788
789

790 **List of Tables**

796

797

798

799

800

801

802

803

804

805

806

807

808

809

810

811

812

List of Figures

840 Figure 16. Infrared spectroscopy of Montmorillonite and organoclays with and without p-
841 nitrophenol in the 1560 ~ 1360 cm^{-1} spectral range

842 Figure 17. Uptake of p-nitrophenol on montmorillonite and organoclays

843

844

845

846

847

848

849

850

851

852

853

854

855

856

857

858

859

860

861

862

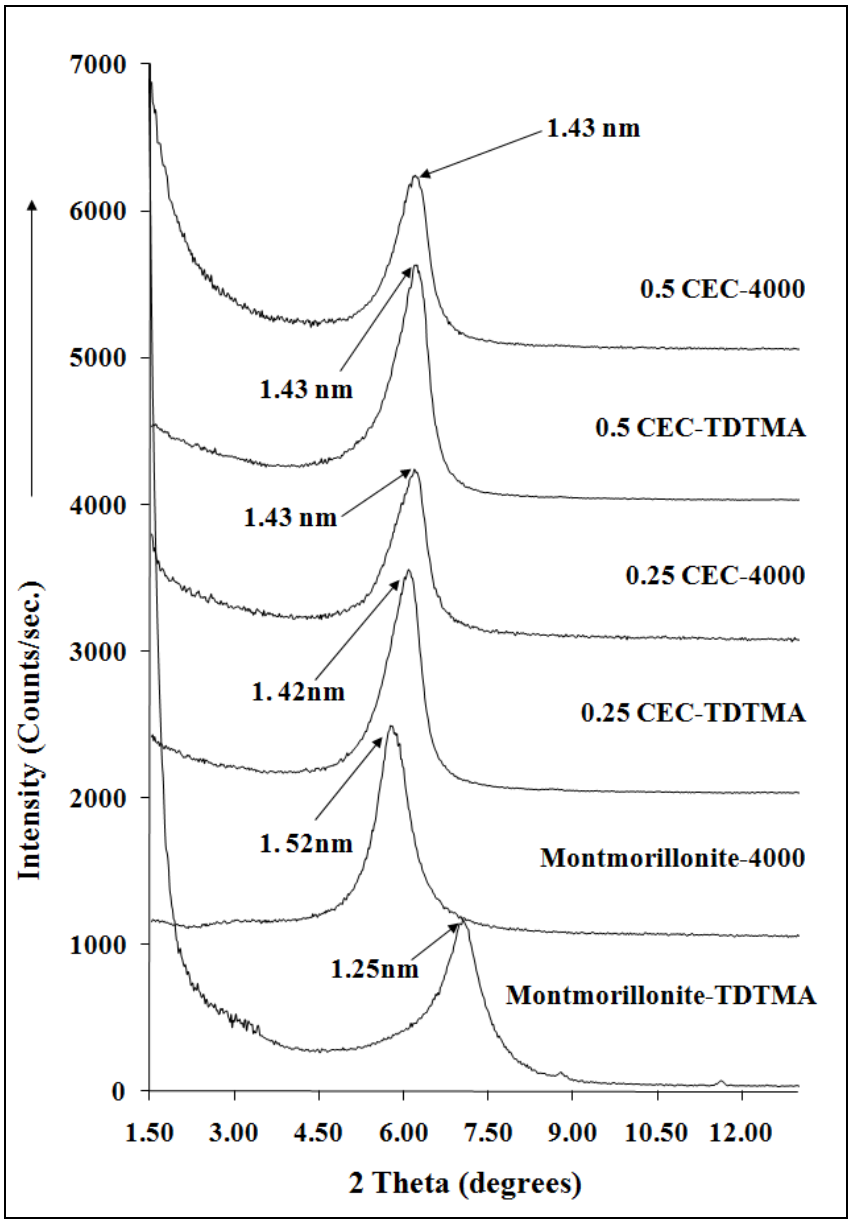

Figure 1 XRD patterns of montmorillonite, 0.25 CEC, and 0.5 CEC with and without adsorbed p-nitrophenol

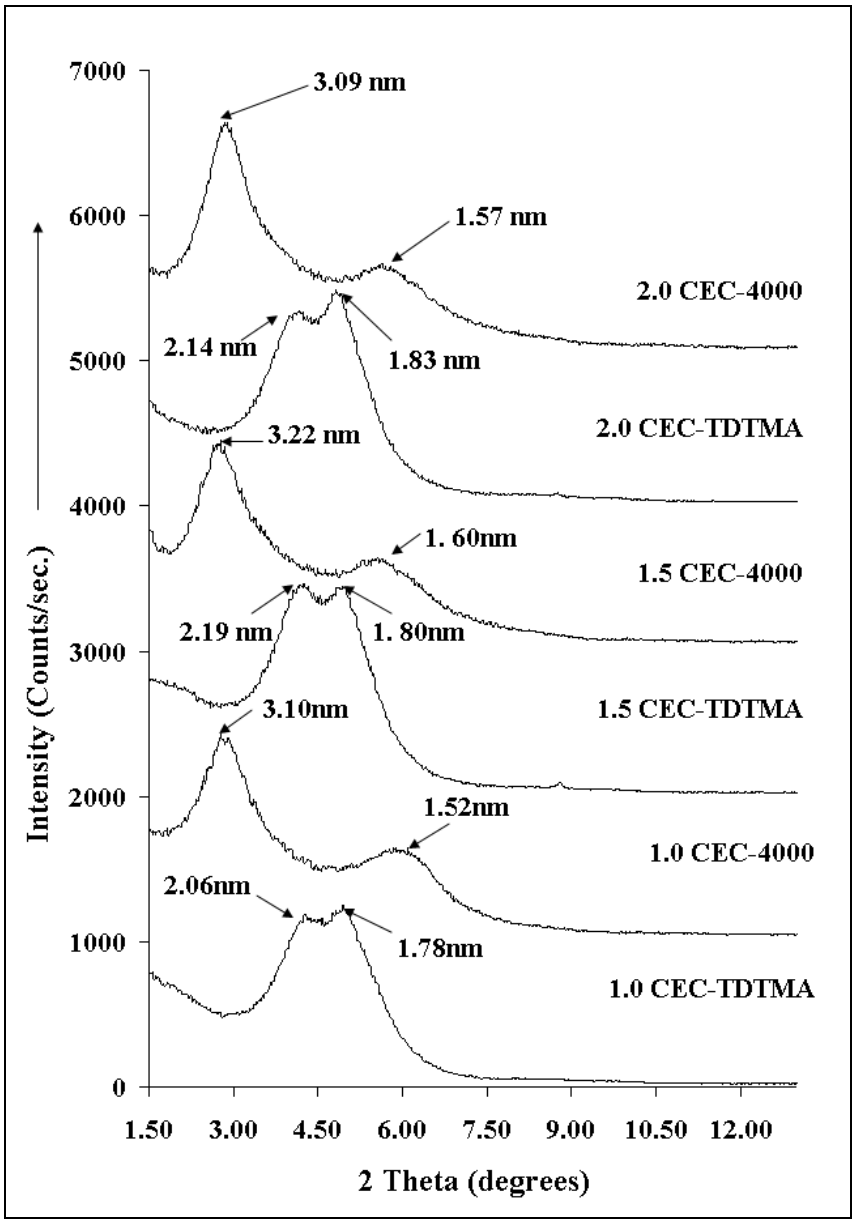

Figure 2 XRD patterns of 1.0 CEC, 1.50 CEC, and 2.0 CEC with and without adsorbed p-nitrophenol

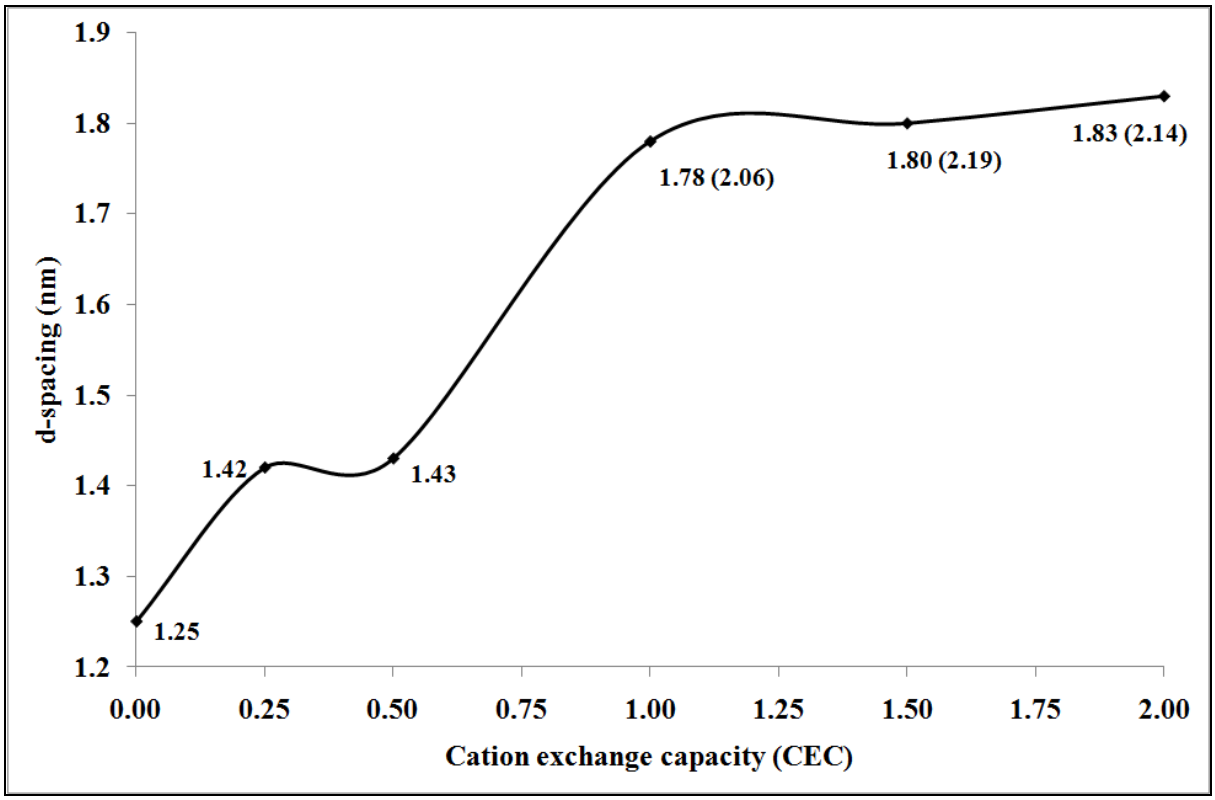

Figure 3 d(001) basal spacing of montmorillonite and organoclays

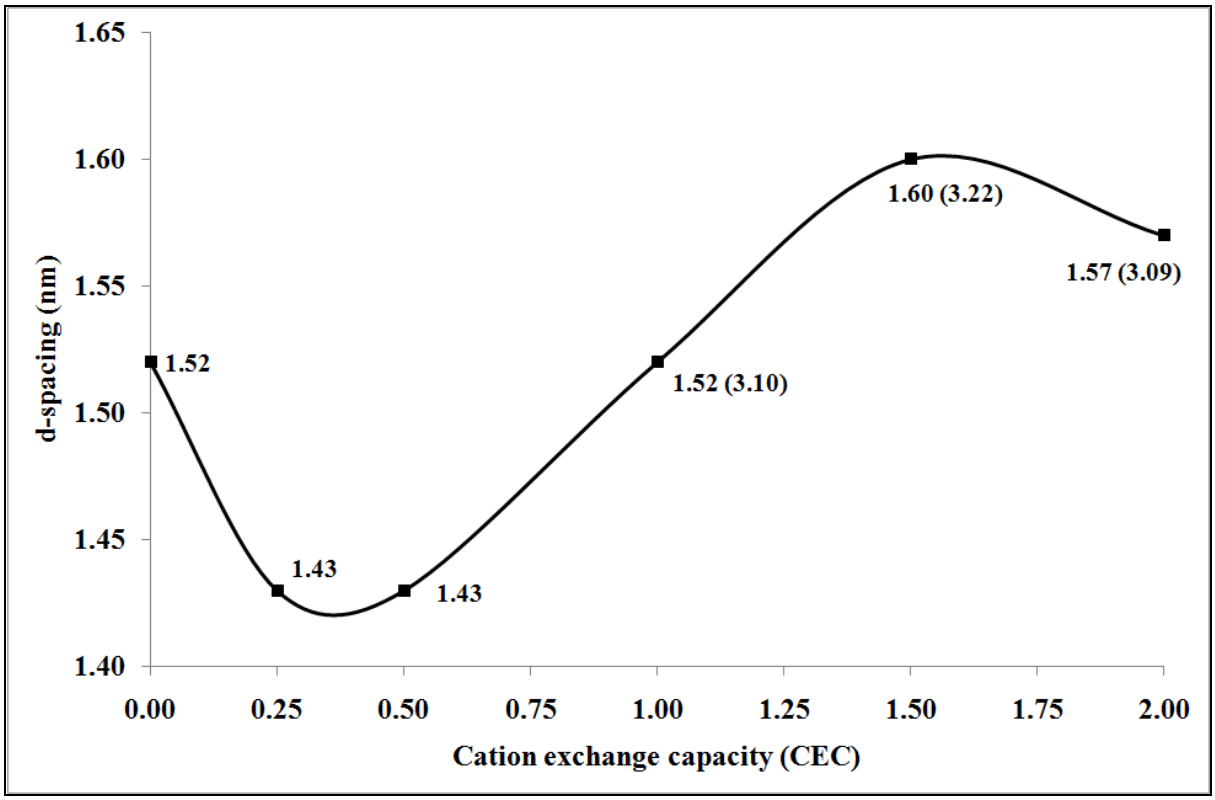

Figure 4 d(001) basal spacing of montmorillonite and organoclays with adsorbed p-nitrophenol

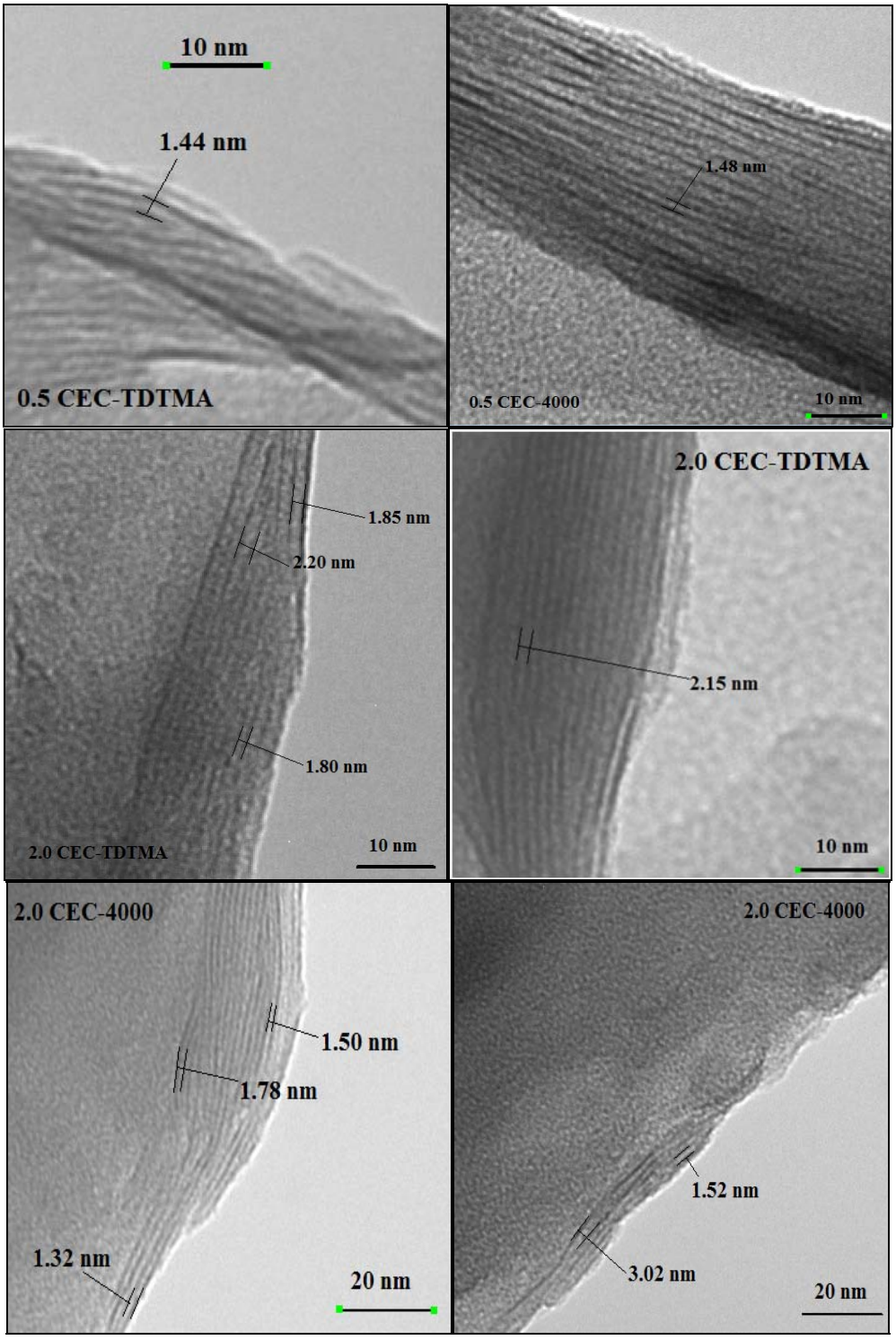

Figure 5 TEM images of 0.5 CEC-TDTMA, 2.0 CEC-TDTMA, 0.5 CEC-4000, and 2.0 CEC-4000

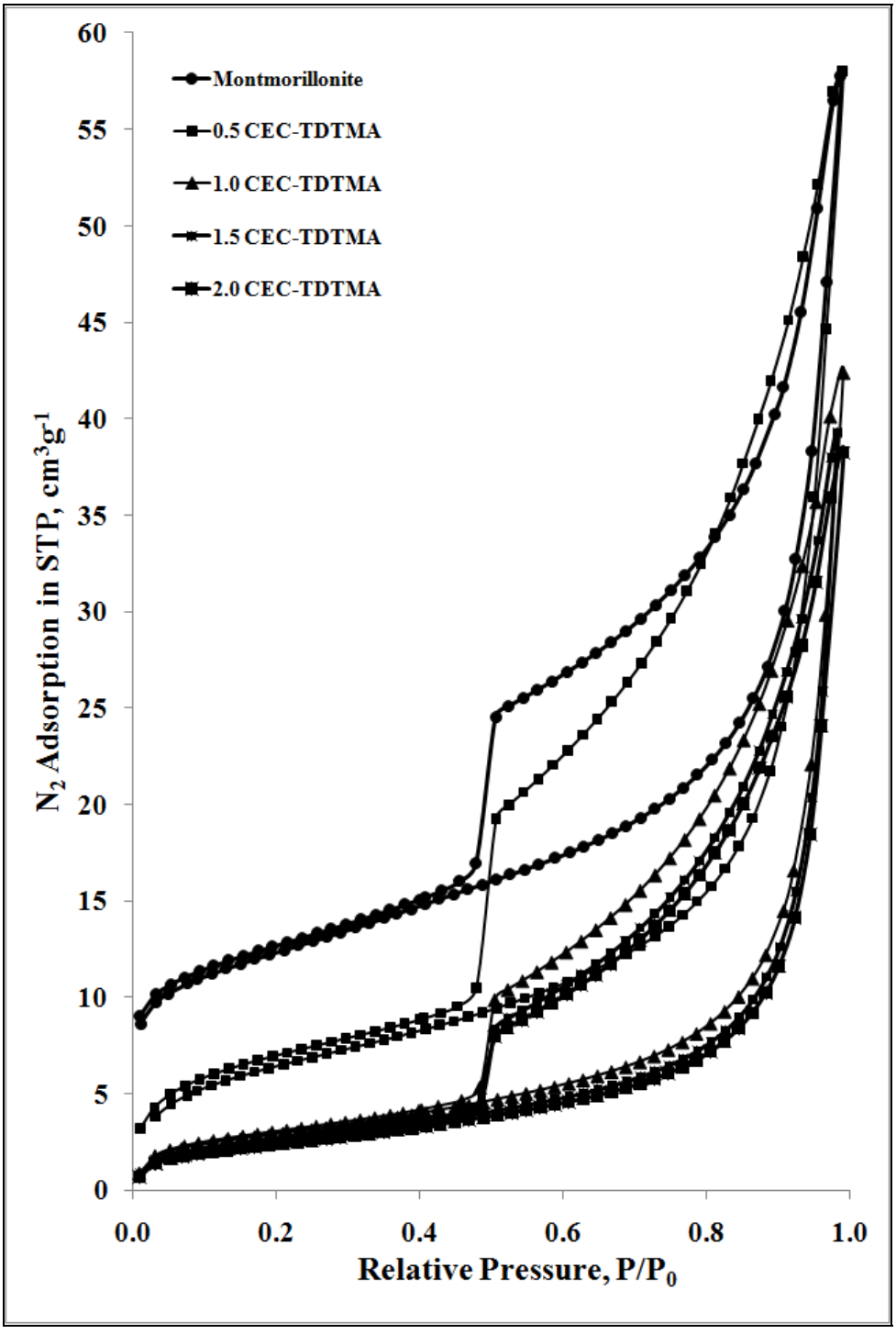

Figure 6 Nitrogen adsorption-desorption isotherms of montmorillonite and organoclays

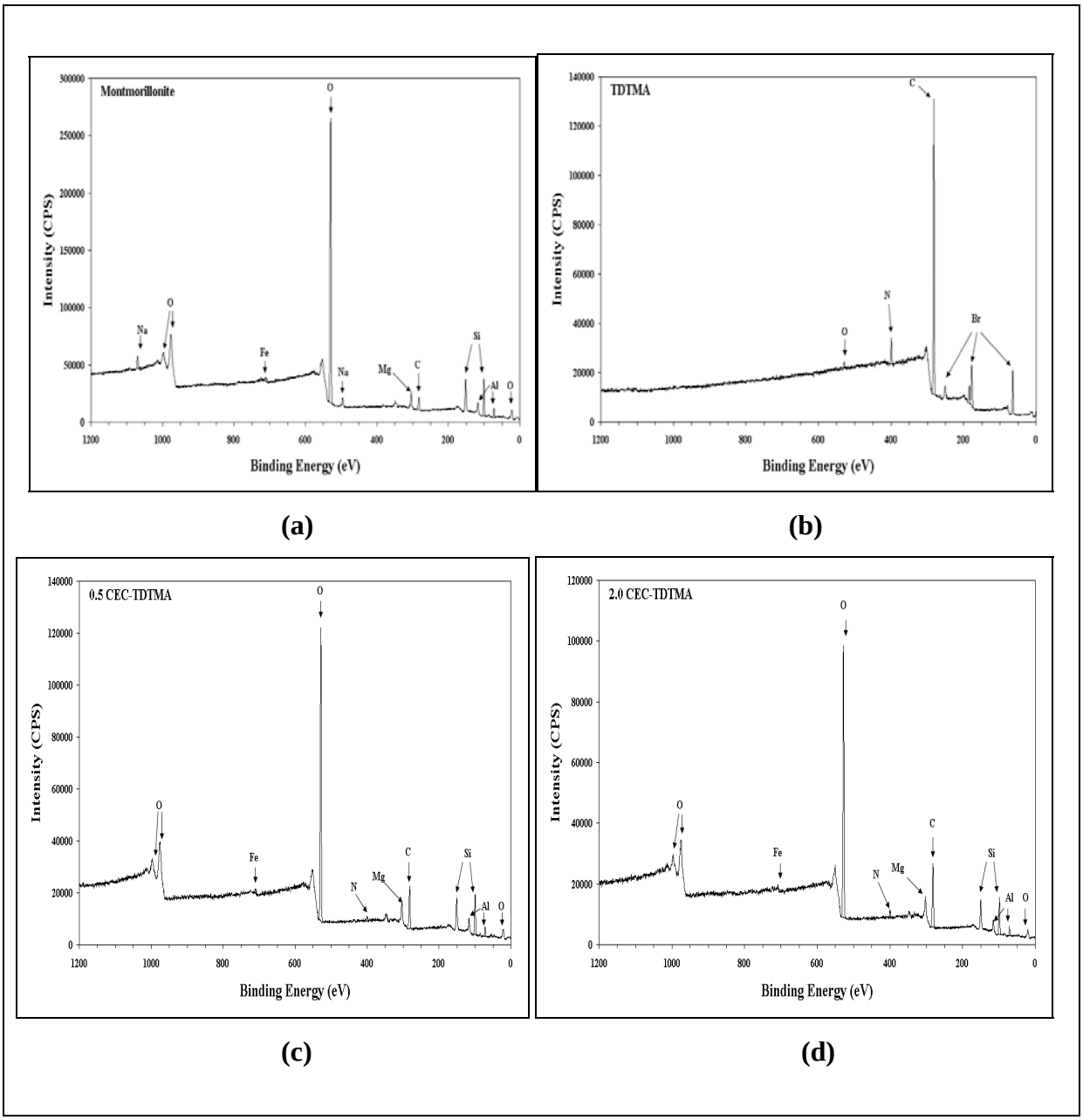

Figure 7 XPS survey scan spectra of montmorillonite (a), surfactant (b), and organoclays (c and d)

930

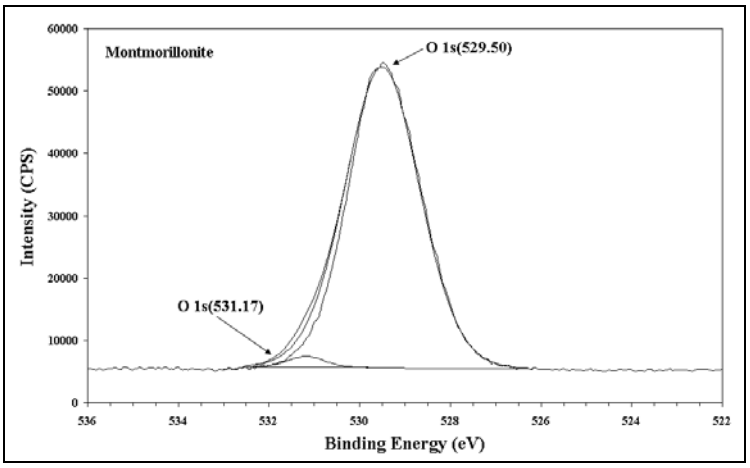

931 **(a)**

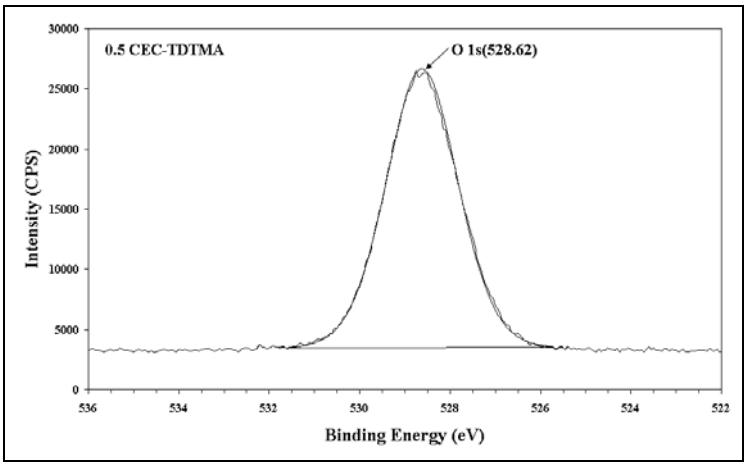

932 **(b)**

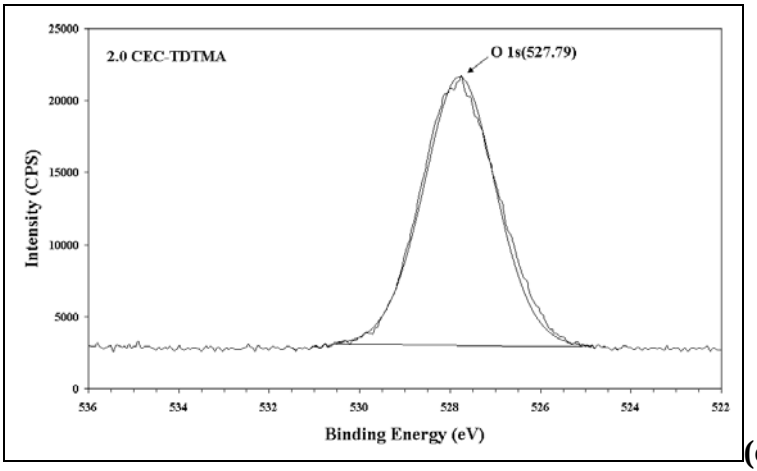

933 **(c)**

934 **Figure 8 XPS high resolution spectra of O 1s for montmorillonite (a), organoclays (b, c)**

935

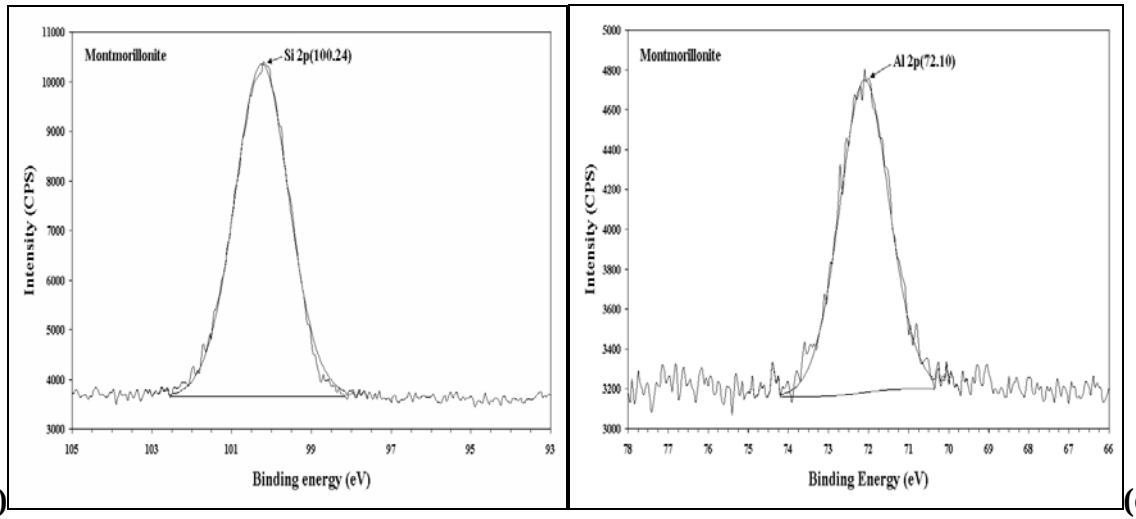

936 **(a)** **(d)**

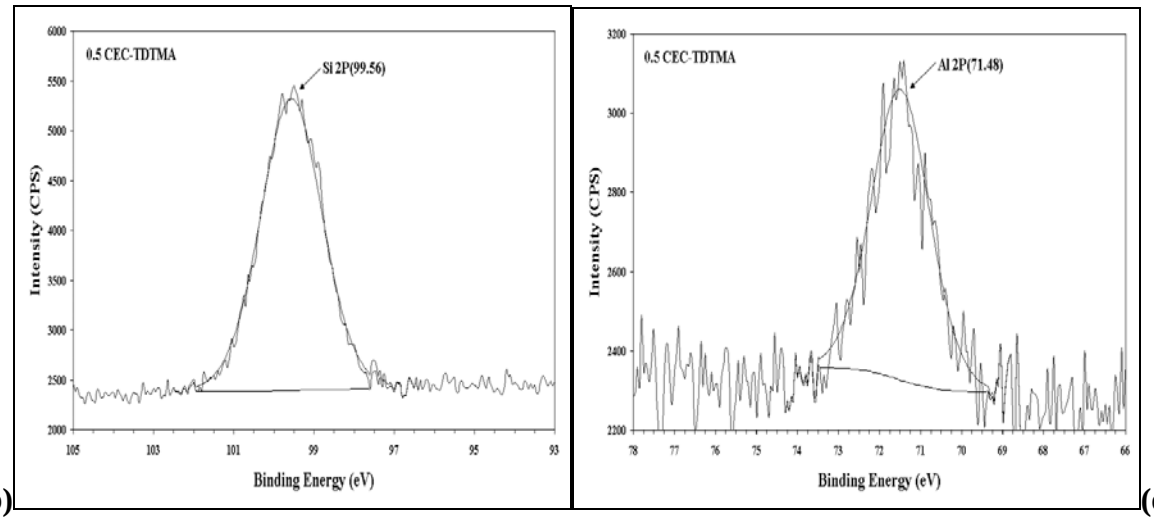

937 **(b)** **(e)**

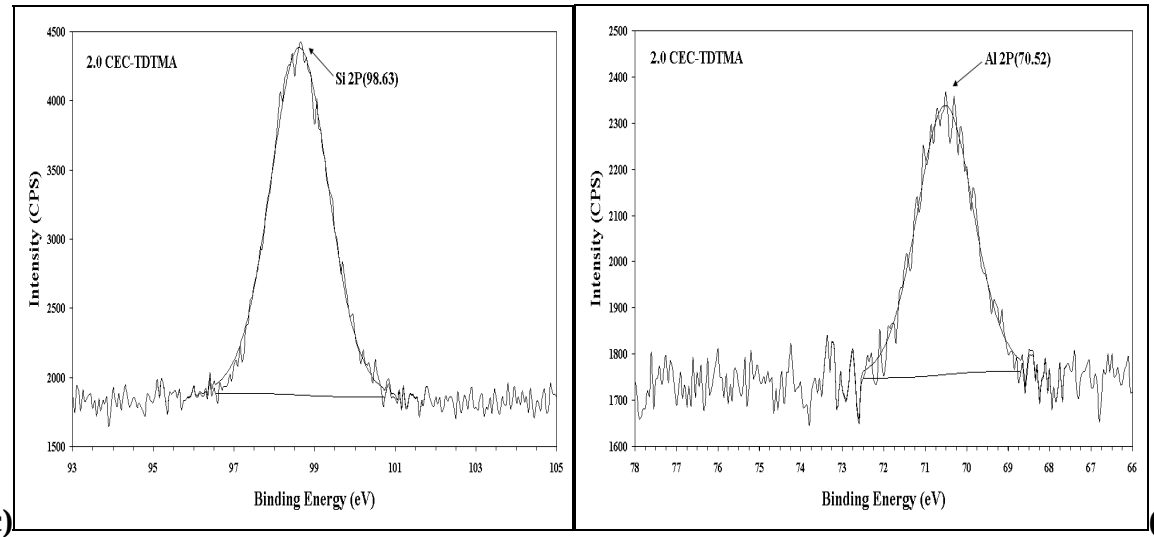

938 **(c)** **(f)**

939 **Figure 9 XPS high resolution spectra of Si 2p and Al 2p for montmorillonite (a and d),**
940 **organoclays (b, e and c, f)**

941

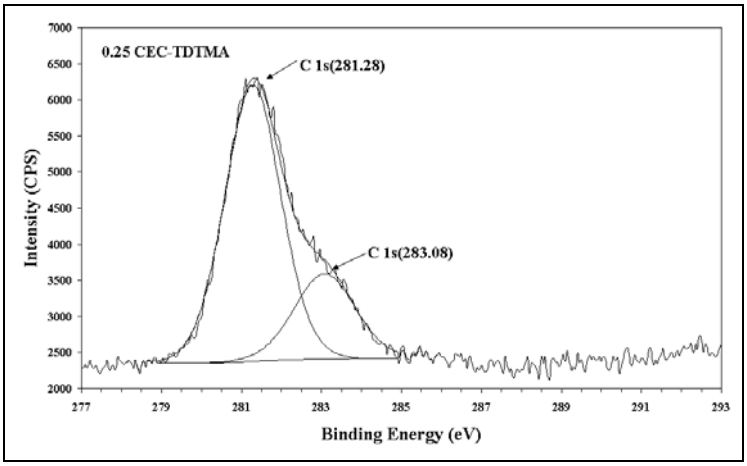

942 **(a)**

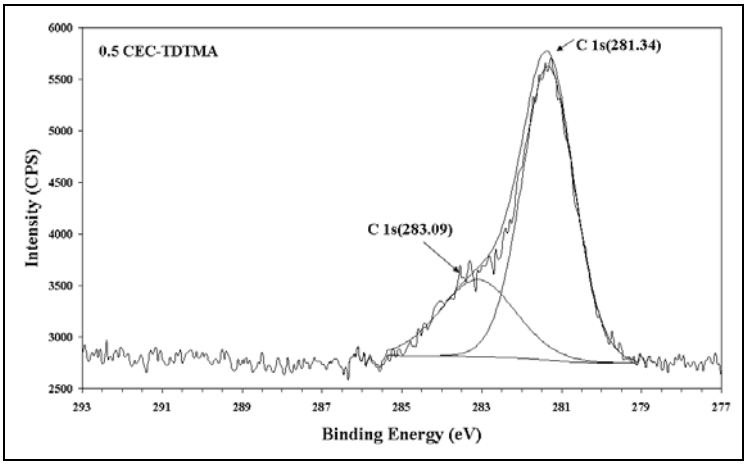

943 **(b)**

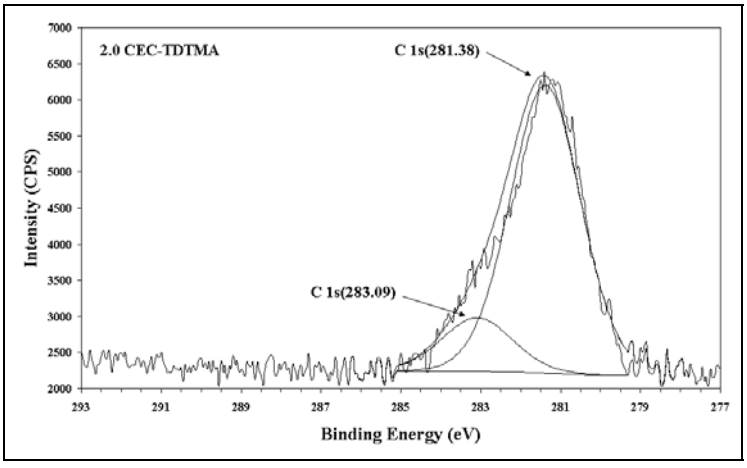

944 **(c)**

945 **Figure 10 XPS high resolution spectra of C 1s for organoclays (a, b, c)**

946

947

948

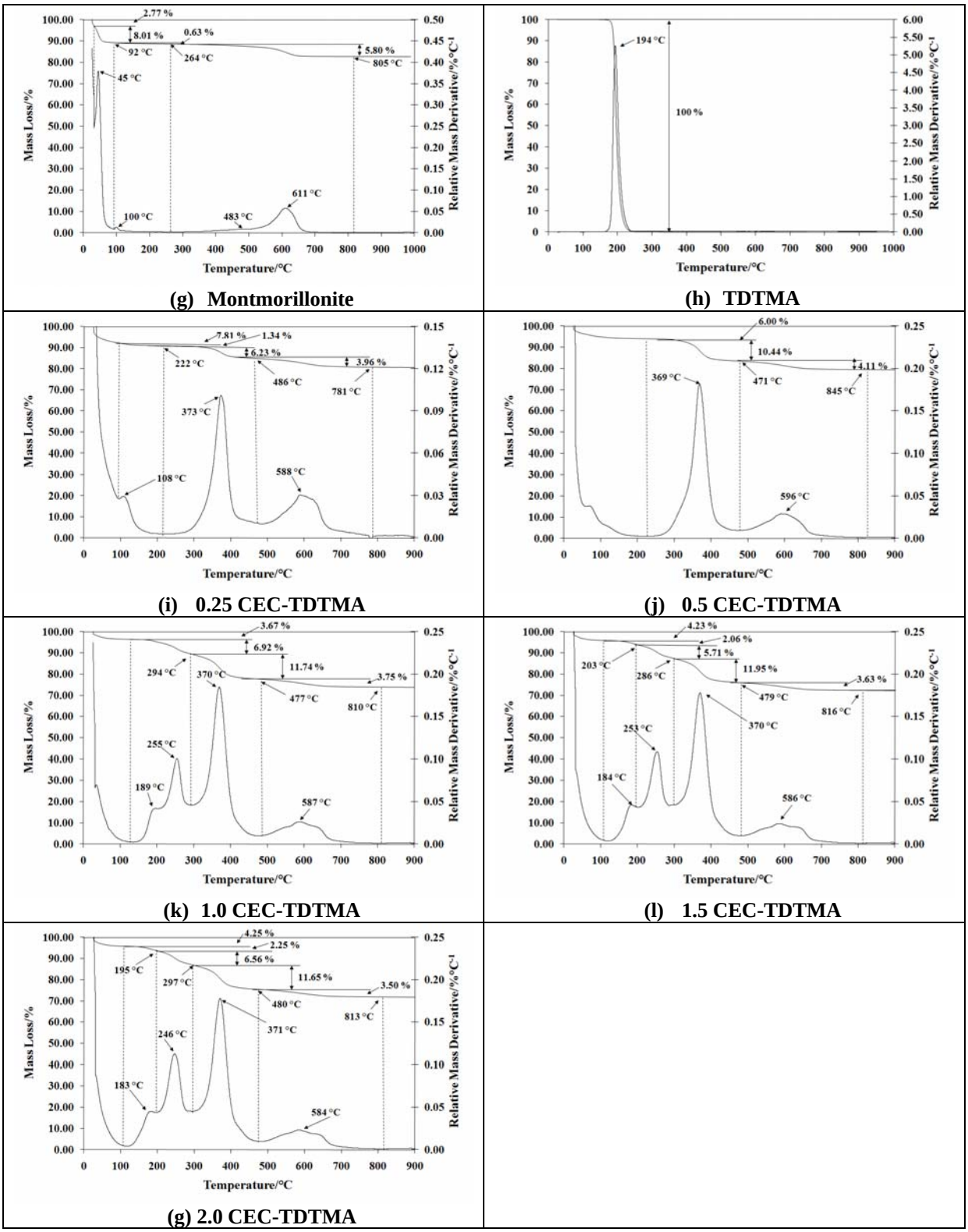

Figure 11 Thermogravimetric analyses of montmorillonite, Surfactant (TDTMA) and organoclays

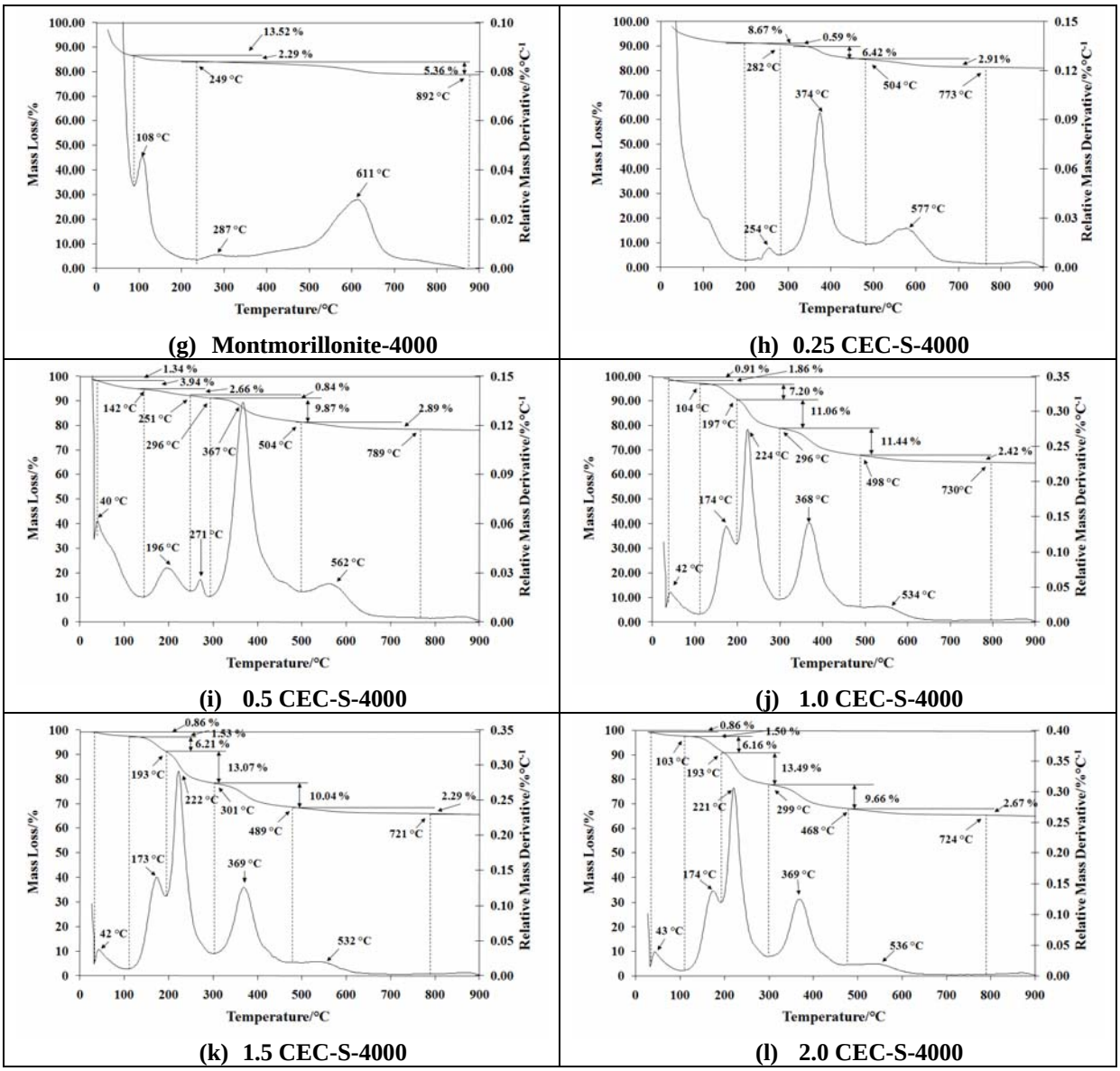

(g) Montmorillonite-4000 **(h) 0.25 CEC-S-4000**

(i) 0.5 CEC-S-4000 **(j) 1.0 CEC-S-4000**

(k) 1.5 CEC-S-4000 **(l) 2.0 CEC-S-4000**

Figure 12 Thermogravimetric analyses of montmorillonite and organoclays adsorbed p-nitrophenol

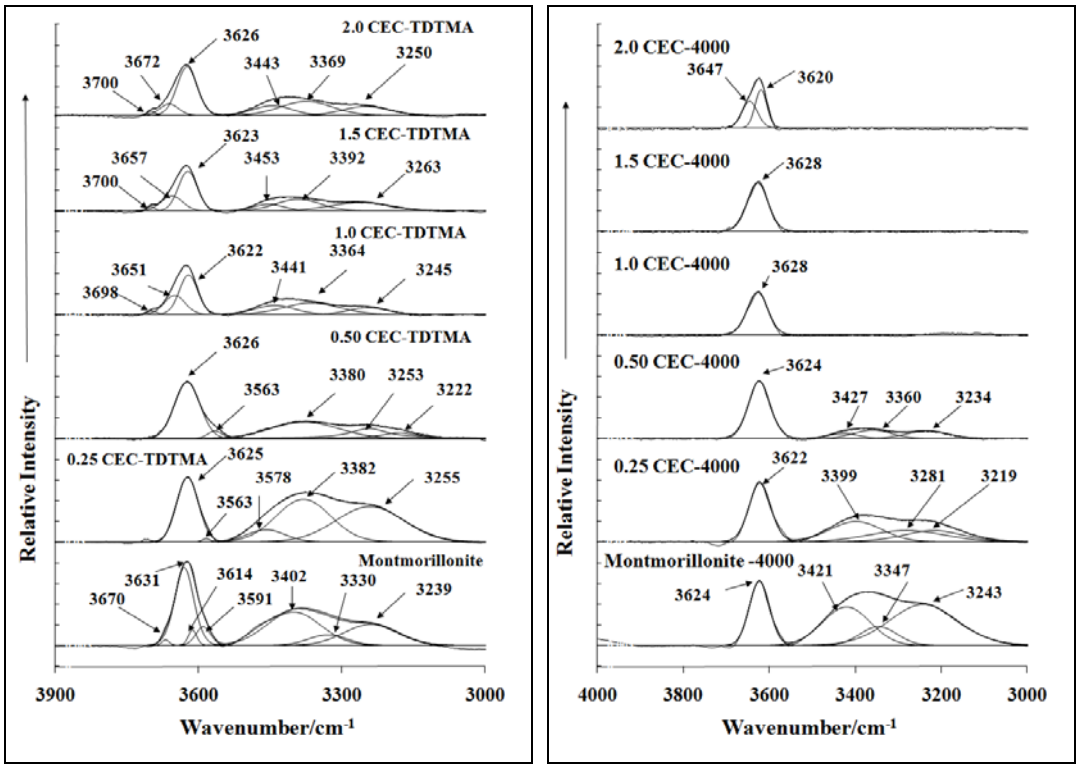

(a) (b)

Figure 13 Infrared spectroscopy of montmorillonite and organoclays with and without p-nitrophenol in 3900 ~ 3000 cm^{-1} spectral range

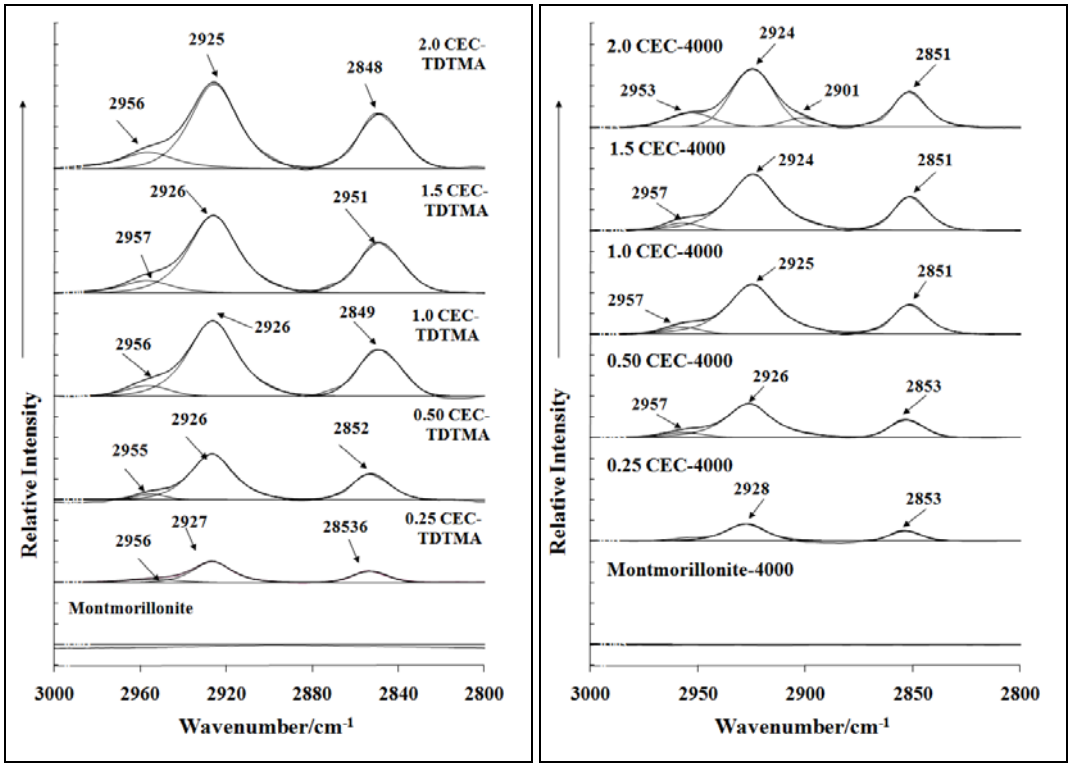

(a) (b)

Figure 14 Infrared spectroscopy of montmorillonite and organoclays with and without p-nitrophenol in the 3000 ~ 2800 cm^{-1} spectral range

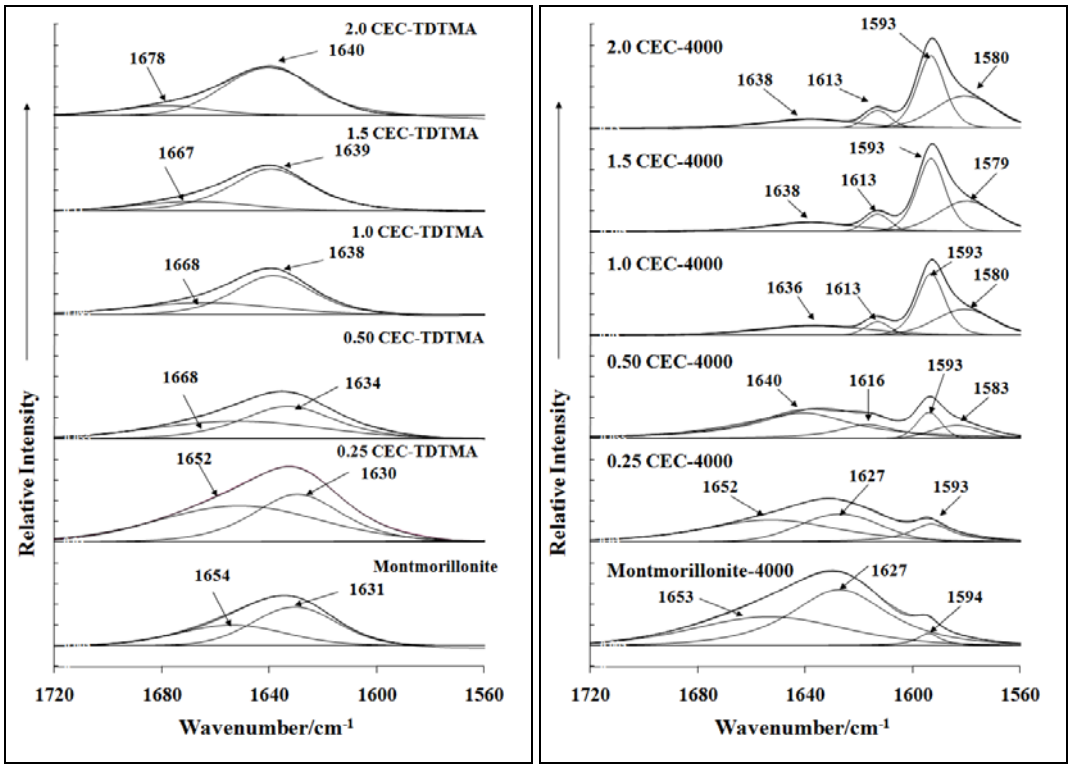

(a) (b)

Figure 15 Infrared spectroscopy of montmorillonite and organoclays with and without p-nitrophenol in the 1720 ~ 1560 cm^{-1} spectral range

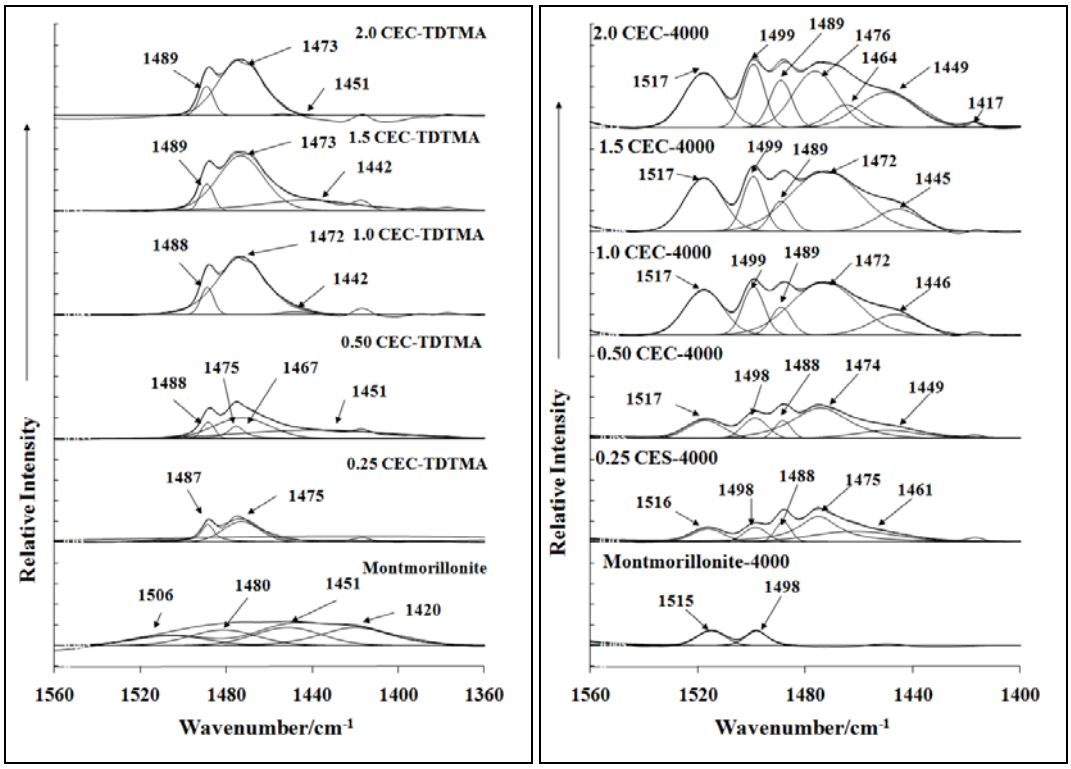

(a) (b)

Figure 16 Infrared spectroscopy of montmorillonite and organoclays without p-nitrophenol in the 1560 ~ 1360 cm^{-1} spectral range

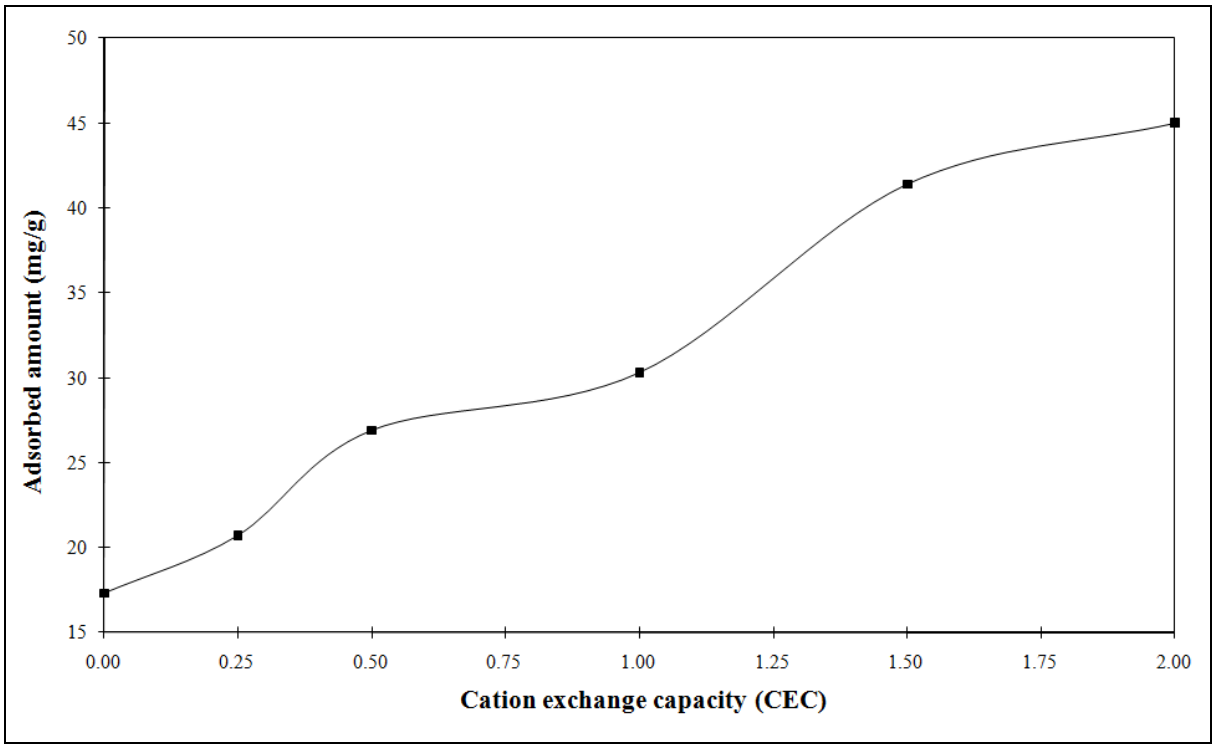

Figure 17. Uptake of p-nitrophenol on montmorillonite and organoclays